Eidgenössische Technische Hochschule Zürich

Ecole polytechnique fédérale de Zurich
Politecnico federale di Zurigo
Swiss Federal Institute of Technology Zurich

Mixed *hp*-DGFEM for incompressible flows II: Geometric edge meshes*

D. Schötzau†, Ch. Schwab and A. Toselli

Research Report No. 2002-21
October 2002

Seminar für Angewandte Mathematik
Eidgenössische Technische Hochschule
CH-8092 Zürich
Switzerland

*This work was partially supported by the Swiss National Science Foundation under Project 20-63397.00

†Department of Mathematics, University of Basel, Rheinsprung 21, CH-4051 Basel, Switzerland, email: `schotzau@math.unibas.ch`

Mixed hp-DGFEM for incompressible flows II: Geometric edge meshes*

D. Schötzau†, Ch. Schwab and A. Toselli

Seminar für Angewandte Mathematik
Eidgenössische Technische Hochschule
CH-8092 Zürich
Switzerland

Research Report No. 2002-21 October 2002

Abstract

We consider the Stokes problem in three-dimensional polyhedral domains discretized on hexahedral meshes with hp-discontinuous Galerkin finite elements of type $\mathbb{Q}_k$ for the velocity and $\mathbb{Q}_{k-1}$ for the pressure. We prove that these elements are inf-sup stable on geometric edge meshes that are refined anisotropically and non quasi-uniformly towards edges and corners. The discrete inf-sup constant is shown to be independent of the aspect ratio of the anisotropic elements and is of order $\mathcal{O}(k^{-3/2})$ in the polynomial degree k, as in the case of $\mathbb{Q}_k$-$\mathbb{Q}_{k-2}$ conforming approximations on the same meshes.

Keywords: hp-FEM, discontinuous Galerkin methods, Stokes problem, geometric edge meshes, anisotropic refinement

Subject Classification: 65N30, 65N35, 65N12, 65N15

---

*This work was partially supported by the Swiss National Science Foundation under Project 20-63397.00

†Department of Mathematics, University of Basel, Rheinsprung 21, CH-4051 Basel, Switzerland, email: `schotzau@math.unibas.ch`

1 Introduction

It is well-known that solutions of elliptic boundary value problems in polyhedral domains have corner and edge singularities. In addition, boundary layers may also arise in laminar, viscous, incompressible flows with moderate Reynolds numbers at faces, edges, and corners. Suitably graded meshes, geometrically refined towards corners, edges, and/or faces, are required in order to achieve an exponential rate of convergence of *hp*-finite element approximations; see, e.g., [3, 5, 23, 28, 29].

The Stokes and Navier-Stokes equations are mixed elliptic systems with saddle point variational structure. The stability and accuracy of the corresponding finite element approximations depend on an inf-sup condition for the finite element spaces that are chosen for the velocities and the pressures. Even for stable velocity-pressure combinations, the corresponding inf-sup constants may in general be very sensitive to the aspect ratio of the mesh, thus degrading the stability if very thin elements are employed, as required for boundary-layer and singularity resolution. It has recently been shown for two- and three-dimensional conforming approximations employing $\mathbb{Q}_k - \mathbb{Q}_{k-2}$ elements, on corner, edge, and boundary-layer tensor-product meshes, that the dependence on the polynomial degree of the inf-sup constant for the Stokes problem might be only slightly worse than that for isotropically refined triangulations but is independent of the aspect ratio of the anisotropic elements; see [24, 25, 1, 33].

Discontinuous Galerkin (DG) approximations rely on discrete spaces consisting of piecewise polynomial functions with no kind of continuity constraints across the interfaces between the elements of a triangulation. They present considerable advantages for certain types of problems, especially those modeling phenomena where convection is moderate or strong; see, e.g., [11, 14, 15] and the references therein. DG approximations often allow for greater flexibility in the design of the mesh and in the choice of the approximation spaces since they do not usually require geometrically conforming triangulations. We note however that even if convection may be the dominant effect of a problem, diffusive terms still need to be accounted for and correctly discretized in a DG framework. Some mixed DG approximations have been proposed. We mention the methods in [6, 22, 13, 12, 20, 19]. In [32, 26], DG *hp*-approximations in two and three dimensions have been proposed and analyzed for tensor product meshes. Numerical evidence hints that DG approximations exhibit better divergence stability properties than the corresponding conforming ones; see [32] for the case of $\mathbb{Q}_k - \mathbb{Q}_k$, $\mathbb{Q}_k - \mathbb{Q}_{k-1}$, and $\mathbb{Q}_k - \mathbb{Q}_{k-2}$ elements.

In this paper, we consider $\mathbb{Q}_k - \mathbb{Q}_{k-1}$ DG approximations in three dimensions. They were originally studied in [32] and then in [26] for shape-regular meshes, possibly with hanging nodes. In particular, it was shown that these approximation spaces are divergence stable uniformly with respect to the mesh size h. The best bound for the inf-sup constant in terms of the polynomial degree k was given in [26] and decreases as k^{-1} both in two and three dimensions. Even though this estimate does not appear to be sharp, at least in two dimensions (see the numerical results in [32]), it ensures the same convergence rate for the velocity and the pressure as that of conforming $\mathbb{Q}_k - \mathbb{Q}_{k-2}$ elements in three dimensions, but with a gap in the polynomial degree of the velocity-pressure pair of just one. We also note that a similar approach was considered in [20] for h-finite element approximations on shape-regular tetrahedral meshes for mixed formulations of elasticity problems.

Here, we generalize our analysis in [26] to the case of geometric edge meshes consisting of hexahedral elements in $\mathbb{R}^3$. These meshes are refined anisotropically and non quasi-uniformly towards edges and corners in order to resolve edge and corner singularities at exponential rates of convergence. We show that the inf-sup constant for discontinuous $\mathbb{Q}_k - \mathbb{Q}_{k-1}$ elements decreases as $Ck^{-3/2}$, with a constant C that only depends on the geometric grading factor, but is independent of the degree k, the level of refinement, and the aspect ratio of the anisotropic elements. We recall that for conforming $\mathbb{Q}_k - \mathbb{Q}_{k-2}$ approximations the inf-sup constant on geometric edge meshes decreases as $Ck^{-1/2}$ in two dimensions and as $Ck^{-3/2}$ in three dimensions; see [24, 25, 33]. The inf-sup constant of our method has thus the same dependence on k as that of conforming approximations, but with an optimal gap of just one order.

In this paper we consider the symmetric interior penalty discontinuous Galerkin method, but note that our stability results remain valid for all the methods discussed in [26]. Moreover, we note that our analysis is also valid for linear elasticity problems in nearly incompressible materials, see, e.g., [9, 16], since the same inf-sup condition is required in order to have approximations that remain stable close to the incompressible limit.

This paper is organized as follows: In section 2, we review the discrete setting from [26] that we use in our stability analysis. Section 3 is devoted to the definition and construction of geometric edge meshes. In section 4, we discuss continuity and coercivity properties of the discontinuous Galerkin forms. Our main stability result is an inf-sup condition for the divergence form on geometric edge meshes and is presented in section 5. In order to prove this result, several ingredients are needed. First, in section 6, we establish a macro-element technique for mixed hp-discontinuous discretizations in the spirit of [31, 24, 25, 33]. This technique allows us to investigate the stability on reference configurations. Then, to address the stability on one of these configurations, namely the edge patch, we provide estimates of Raviart-Thomas interpolants on stretched elements in section 7. The stability on edge patches is shown in section 8. Finally, we complete the proof of our stability result in section 9.

2 Mixed hp-DGFEM for the Stokes problem

In this section, we introduce mixed hp-discontinuous Galerkin methods for the Stokes problem in incompressible fluid flow, and review the theoretical framework of [26] that we use to analyze the methods on geometric edge meshes.

2.1 The Stokes equations

Let Ω be a bounded polyhedral domain in $\mathbb{R}^3$, with $\mathbf{n}$ denoting the outward normal unit vector to its boundary $\partial\Omega$. Given a source term $\mathbf{f} \in L^2(\Omega)^3$ and a Dirichlet datum $\mathbf{g} \in H^{1/2}(\partial\Omega)^3$ satisfying the compatibility condition $\int_{\partial\Omega} \mathbf{g} \cdot \mathbf{n}\, ds = 0$, the Stokes problem for incompressible fluid flows consists in finding a velocity field $\mathbf{u}$ and a pressure p such that

$$\begin{aligned} -\nu\Delta\mathbf{u} + \nabla p &= \mathbf{f} && \text{in } \Omega, \\ \nabla \cdot \mathbf{u} &= 0 && \text{in } \Omega, \\ \mathbf{u} &= \mathbf{g} && \text{on } \partial\Omega. \end{aligned} \tag{1}$$

By setting $\mathbf{V} := H^1(\Omega)^3$, $Q := L^2_0(\Omega) = \{\, q \in L^2(\Omega) : \int_\Omega q\, d\mathbf{x} = 0 \,\}$ and

$$A(\mathbf{u}, \mathbf{v}) = \int_\Omega \nu\nabla\mathbf{u} : \nabla\mathbf{v}\, d\mathbf{x}, \qquad B(\mathbf{v}, q) = -\int_\Omega q\, \nabla \cdot \mathbf{v}\, d\mathbf{x},$$

we obtain the usual mixed variational formulation of the Stokes problem that consists in finding $(\mathbf{u}, p) \in \mathbf{V} \times Q$, with $\mathbf{u} = \mathbf{g}$ on $\partial\Omega$, such that

$$\left\{ \begin{array}{lclcl} A(\mathbf{u}, \mathbf{v}) & + & B(\mathbf{v}, p) & = & \int_\Omega \mathbf{f} \cdot \mathbf{v}\, d\mathbf{x} \\ B(\mathbf{u}, q) & & & = & 0 \end{array} \right. \tag{2}$$

for all $\mathbf{v} \in H^1_0(\Omega)^3$ and $q \in Q$. As usual, $H^1_0(\Omega)^3$ is the subspace of $H^1(\Omega)^3$ of vectors that vanish on $\partial\Omega$.

The well-posedness of (2) is ensured by the continuity of $A(\cdot, \cdot)$ and $B(\cdot, \cdot)$, the coercivity of $A(\cdot, \cdot)$, and the following inf-sup condition

$$\inf_{0 \neq q \in L^2_0(\Omega)} \sup_{\mathbf{0} \neq \mathbf{v} \in H^1_0(\Omega)^d} \frac{B(\mathbf{v}, q)}{|\mathbf{v}|_1 \|q\|_0} \geq \gamma_\Omega > 0, \tag{3}$$

with an inf-sup constant γ_Ω only depending on Ω; see, e.g., [9, 18]. Here, we denote by $\|\cdot\|_{s,\mathcal{D}}$ and $|\cdot|_{s,\mathcal{D}}$ the norm and seminorm of $H^s(\mathcal{D})$ and $H^s(\mathcal{D})^3$, $s \geq 0$. In case $\mathcal{D} = \Omega$, we drop the subscript.

2.2 Meshes and trace operators

Throughout, we consider meshes $\mathcal{T}$ in two and three space dimensions that consist of quadrilaterals and hexahedra $\{K\}$, respectively. Each element $K \in \mathcal{T}$ is affinely equivalent to a reference element $\widehat{K}$, which is either the reference square $\widehat{S} = (-1, 1)^2$ or the reference cube $\widehat{Q} = (-1, 1)^3$. The edges of $\widehat{S}$ and the faces of $\widehat{Q}$ are denoted by $\widehat{f}_m$, $m = 1, \ldots, 2d$, $d = 2, 3$, where

$$\begin{array}{lll} \widehat{f}_1 = \{x = -1\}, & \widehat{f}_2 = \{x = 1\}, & \\ \widehat{f}_3 = \{y = -1\}, & \widehat{f}_4 = \{y = 1\}, & \\ \widehat{f}_5 = \{z = -1\}, & \widehat{f}_6 = \{z = 1\}, & d = 3. \end{array}$$

We write $\{f_i\}_{i=1}^{2d}$ to denote the edges or faces of an element $K \in \mathcal{T}$; they are obtained by mapping the corresponding ones of $\widehat{K}$. In general, we allow for *irregular* meshes, i.e., meshes with so-called hanging nodes (see [27, Sect. 4.4.1]), but suppose that the intersection between neighboring elements is a vertex, an edge, or a face (if $d = 3$) of at least one of the two elements. For an element $K \in \mathcal{T}$, we denote by h_K the diameter and by ρ_K the radius of the biggest circle or sphere that can be inscribed into K. A mesh $\mathcal{T}$ is called *shape-regular* if

$$h_K \leq c\rho_K, \qquad \forall K \in \mathcal{T}, \tag{4}$$

for a shape-regularity constant $c > 0$ that is independent of the elements. Our meshes are not necessarily shape-regular; see section 3.

Let now $\mathcal{T}$ be a hexahedral mesh on Ω. An interior face of $\mathcal{T}$ is the (non-empty) two–dimensional interior of $\partial K^+ \cap \partial K^-$, where K^+ and K^- are two adjacent elements of $\mathcal{T}$. Similarly, a boundary face of $\mathcal{T}$ is the (non-empty) two-dimensional interior of $\partial K \cap \partial\Omega$ which consists of entire faces of ∂K. We denote by $\mathcal{E}_\mathcal{I}$ the union of all interior faces of $\mathcal{T}$, by $\mathcal{E}_\mathcal{B}$ the union of all boundary faces, and set $\mathcal{E} = \mathcal{E}_\mathcal{I} \cup \mathcal{E}_\mathcal{B}$.

On $\mathcal{E}$, we define the following trace operators. First, let $f \subset \mathcal{E}_\mathcal{I}$ be an interior face shared by two elements K^+ and K^-. Let $\mathbf{v}$, q, and $\underline{\tau}$ be vector-, scalar- and matrix-valued functions, respectively, that are smooth inside each element $K^\pm$, and let us denote by $\mathbf{v}^\pm$, $q^\pm$ and $\underline{\tau}^\pm$ the traces of $\mathbf{v}$, q and $\underline{\tau}$ on f from the interior of $K^\pm$. We define the mean values and the normal jumps at $\mathbf{x} \in f$ as

$$\begin{aligned}
\{\!\{\mathbf{v}\}\!\} &:= (\mathbf{v}^+ + \mathbf{v}^-)/2, & [\![\mathbf{v}]\!] &:= \mathbf{v}^+ \cdot \mathbf{n}_{K^+} + \mathbf{v}^- \cdot \mathbf{n}_{K^-}, \\
\{\!\{q\}\!\} &:= (q^+ + q^-)/2, & [\![q]\!] &:= q^+\, \mathbf{n}_{K^+} + q^-\, \mathbf{n}_{K^-}, \\
\{\!\{\underline{\tau}\}\!\} &:= (\underline{\tau}^+ + \underline{\tau}^-)/2, & [\![\underline{\tau}]\!] &:= \underline{\tau}^+\, \mathbf{n}_{K^+} + \underline{\tau}^-\, \mathbf{n}_{K^-}.
\end{aligned}$$

Here, we denote by $\mathbf{n}_K$ the outward normal unit vector to the boundary ∂K of an element K. We also need to define the matrix-valued jump of $\mathbf{v}$, namely,

$$\underline{[\![\mathbf{v}]\!]} := \mathbf{v}^+ \otimes \mathbf{n}_{K^+} + \mathbf{v}^- \otimes \mathbf{n}_{K^-},$$

where, for two vectors $\mathbf{a}$ and $\mathbf{b}$, $[\mathbf{a} \otimes \mathbf{b}]_{ij} = a_i b_j$. On a boundary face $f \subset \mathcal{E}_\mathcal{B}$ given by $f = \partial K \cap \partial\Omega$, we then set accordingly $\{\!\{\mathbf{v}\}\!\} := \mathbf{v}$, $\{\!\{q\}\!\} := q$, $\{\!\{\underline{\tau}\}\!\} := \underline{\tau}$, as well as $[\![\mathbf{v}]\!] := \mathbf{v} \cdot \mathbf{n}$, $\underline{[\![\mathbf{v}]\!]} := \mathbf{v} \otimes \mathbf{n}$, $[\![q]\!] := q\mathbf{n}$ and $[\![\tau]\!] := \tau \cdot \mathbf{n}$.

2.3 Finite element spaces

For a mesh $\mathcal{T}$ on a polyhedron $\mathcal{D}$ and an approximation order $k \geq 0$, we introduce the finite element spaces

$$\begin{aligned}
\mathbf{V}_h^k(\mathcal{T}; \mathcal{D}) &:= \{\, \mathbf{v} \in L^2(\mathcal{D})^3 : \mathbf{v}|_K \in \mathbb{Q}_k(K)^3,\ K \in \mathcal{T} \,\}, \\
Q_h^k(\mathcal{T}; \mathcal{D}) &:= \{\, q \in L^2(\mathcal{D}) : q|_K \in \mathbb{Q}_k(K),\ K \in \mathcal{T},\ \int_\mathcal{D} q d\mathbf{x} = 0 \,\},
\end{aligned}$$

where $\mathbb{Q}_k(K)$ is the space of polynomials of maximum degree k in each variable on the element K. Further, we define the subspace $\widetilde{\mathbf{V}}_h^k(\mathcal{T};\mathcal{D})$ of $\mathbf{V}_h^k(\mathcal{T};\mathcal{D})$ of vectors with vanishing normal component on the boundary of $\mathcal{D}$

$$\widetilde{\mathbf{V}}_h^k(\mathcal{T};\mathcal{D}) = \{\, \mathbf{v} \in \mathbf{V}_h^k(\mathcal{T};\mathcal{D}) : \mathbf{v}\cdot\mathbf{n}_{\mathcal{D}} = 0 \text{ on } \partial\mathcal{D} \,\},$$

with $\mathbf{n}_{\mathcal{D}}$ denoting the outward normal unit vector to $\partial\mathcal{D}$. For $\mathcal{D} = \Omega$, we omit the dependence on the domain and simply write $\mathbf{V}_h^k(\mathcal{T})$, $Q_h^k(\mathcal{T})$ and $\widetilde{V}_h^k(\mathcal{T})$.

2.4 Mixed discontinuous Galerkin approximations

For a mesh $\mathcal{T}$ on Ω, we approximate the velocities and pressures in the spaces $\mathbf{V}_h$ and Q_h given by

$$\mathbf{V}_h := \mathbf{V}_h^k(\mathcal{T}), \qquad Q_h := Q_h^{k-1}(\mathcal{T}), \qquad k \geq 1.$$

We refer to this velocity-pressure pair as (non-conforming) $\mathbb{Q}_k - \mathbb{Q}_{k-1}$ elements.

In order to apply the framework of [26], we need to define the additional space $\mathbf{V}(h) := \mathbf{V} + \mathbf{V}_h$, endowed with the broken norm

$$\|\mathbf{v}\|_h^2 := \sum_{K\in\mathcal{T}} |\mathbf{v}|_{1,K}^2 + \int_{\mathcal{E}} \delta |\underline{[\![\mathbf{v}]\!]}|^2 \, ds, \qquad \mathbf{v} \in \mathbf{V}(h).$$

Here, $\delta \in L^\infty(\mathcal{E})$ is the so-called discontinuity stabilization function, for which we will make a precise choice in section 3.2 below. Further, we define the lifting operators

$$\int_\Omega \underline{\mathcal{L}}(\mathbf{v}) : \underline{\tau} \, d\mathbf{x} = \int_{\mathcal{E}} \underline{[\![\mathbf{v}]\!]} : \{\!\{\underline{\tau}\}\!\} \, ds \qquad \forall \underline{\tau} \in \underline{\Sigma}_h, \tag{5}$$

$$\int_\Omega \mathcal{M}(\mathbf{v}) q \, d\mathbf{x} = \int_{\mathcal{E}} [\![\mathbf{v}]\!] \{\!\{q\}\!\} \, ds \qquad \forall q \in Q_h, \tag{6}$$

where we use the auxiliary space $\underline{\Sigma}_h := \{\, \underline{\tau} \in L^2(\Omega)^{3\times 3} : \underline{\tau}|_K \in \mathbb{Q}_k(K)^{3\times 3},\ K \in \mathcal{T} \,\}$.

We consider the following mixed DG method: find $(\mathbf{u}_h, p_h) \in \mathbf{V}_h \times Q_h$ such that

$$\left\{ \begin{array}{lcllcl} A_h(\mathbf{u}_h, \mathbf{v}) & + & B_h(\mathbf{v}, p_h) & = & F_h(\mathbf{v}) \\ B_h(\mathbf{u}_h, q) & & & = & G_h(q) \end{array} \right. \tag{7}$$

for all $(\mathbf{v}, q) \in \mathbf{V}_h \times Q_h$. Here, $A_h : \mathbf{V}(h) \times \mathbf{V}(h) \to \mathbb{R}$ and $B_h : \mathbf{V}(h) \times Q \to \mathbb{R}$ are the following forms:

$$\begin{aligned} A_h(\mathbf{u}, \mathbf{v}) &= \int_\Omega \nu \big[\nabla_h \mathbf{u} : \nabla_h \mathbf{v} - \underline{\mathcal{L}}(\mathbf{u}) : \nabla_h \mathbf{v} - \underline{\mathcal{L}}(\mathbf{v}) : \nabla_h \mathbf{u} \big] \, d\mathbf{x} \\ &\quad + \nu \int_{\mathcal{E}} \delta \underline{[\![\mathbf{u}]\!]} : \underline{[\![\mathbf{v}]\!]} \, ds, \\ B_h(\mathbf{v}, q) &= - \int_\Omega q \, [\nabla_h \cdot \mathbf{v} - \mathcal{M}(\mathbf{v})] \, d\mathbf{x}, \end{aligned} \tag{8}$$

where ∇_h is the discrete gradient, taken elementwise. The right-hand sides $F_h : \mathbf{V}_h \to \mathbb{R}$ and $G_h : Q_h \to \mathbb{R}$ are given by

$$\begin{aligned} F_h(\mathbf{v}) &= \int_\Omega \mathbf{f} \cdot \mathbf{v}\, d\mathbf{x} - \int_{\mathcal{E}_\mathcal{B}} (\mathbf{g} \otimes \mathbf{n}) : \{\!\{\nu \nabla_h \mathbf{v}\}\!\}\, ds + \nu \int_{\mathcal{E}_\mathcal{B}} \delta \mathbf{g} \cdot \mathbf{v}\, ds, \\ G_h(q) &= \int_{\mathcal{E}_\mathcal{B}} q\, \mathbf{g} \cdot \mathbf{n}\, ds. \end{aligned}$$

Restricted to discrete functions in $\mathbf{V}_h$ and Q_h, we have

$$\begin{aligned} A_h(\mathbf{u}, \mathbf{v}) &= \int_\Omega \nu \nabla_h \mathbf{u} : \nabla_h \mathbf{v}\, d\mathbf{x} - \int_\mathcal{E} \left(\{\!\{\nu \nabla_h \mathbf{v}\}\!\} : \underline{[\![\mathbf{u}]\!]} + \{\!\{\nu \nabla_h \mathbf{u}\}\!\} : \underline{[\![\mathbf{v}]\!]} \right) ds \\ &\quad + \nu \int_\mathcal{E} \delta \underline{[\![\mathbf{u}]\!]} : \underline{[\![\mathbf{v}]\!]}\, ds, \\ B_h(\mathbf{v}, q) &= - \int_\Omega q\, \nabla_h \cdot \mathbf{v}\, d\mathbf{x} + \int_\mathcal{E} \{\!\{q\}\!\} [\![\mathbf{v}]\!]\, ds. \end{aligned}$$

We note that for $q \in Q_h$

$$B_h(\mathbf{v}, q) = B(\mathbf{v}, q) = - \int_\Omega q\, \nabla \cdot \mathbf{v}\, d\mathbf{x}, \quad \mathbf{v} \in \mathbf{V}_h \cap H_0(\mathrm{div}; \Omega), \tag{9}$$

where the space $H_0(\mathrm{div}; \Omega)$ consists of square-integrable vectors with square-integrable divergence and vanishing normal component on $\partial\Omega$. We note that $\mathbf{V}_h \cap H_0(\mathrm{div}; \Omega)$ consists of discrete vectors with continuous normal component across the interelement boundaries and vanishing normal component on $\partial\Omega$; see, e.g., [9, Ch. III.3].

Remark 2.1. *The form B_h and the functional G_h are exactly those considered in the mixed DG approaches in [13, 20, 32, 26]. The form A_h in (8) is the so-called interior penalty (IP) form. Several other choices are possible for A_h, as discussed in [26]. All the results of this paper hold verbatim for these other forms as well.*

2.5 Well-posedness and error estimates

Problem (7) was analyzed in [26] where an abstract framework was introduced. To the knowledge of the authors, all available mixed DG methods for the Stokes problem can be studied in this framework.

We assume that the forms A_h and B_h satisfy the following continuity properties

$$A_h(\mathbf{u}, \mathbf{v}) \le \alpha_1 \|\mathbf{u}\|_h \|\mathbf{v}\|_h, \qquad \mathbf{u}, \mathbf{v} \in \mathbf{V}(h), \tag{10}$$

$$B_h(\mathbf{v}, q) \le \alpha_2 \|\mathbf{v}\|_h \|q\|_0, \qquad (\mathbf{v}, q) \in \mathbf{V}(h) \times Q, \tag{11}$$

with constants $\alpha_1 > 0$ and $\alpha_2 > 0$, and that A_h is coercive

$$A_h(\mathbf{u}, \mathbf{u}) \ge \beta \|\mathbf{u}\|_h^2, \qquad \mathbf{u} \in \mathbf{V}_h, \tag{12}$$

for a constant $\beta > 0$. Further, we suppose that the following discrete inf-sup condition for the finite element spaces $\mathbf{V}_h$ and Q_h (also referred to as divergence stability) holds true:

$$\inf_{0\neq q\in Q_h} \sup_{\mathbf{0}\neq\mathbf{v}\in\mathbf{V}_h} \frac{B_h(\mathbf{v},q)}{\|\mathbf{v}\|_h\|q\|_0} \geq \gamma_h > 0. \tag{13}$$

The above conditions ensure the well-posedness of (7): Indeed, (7) has a unique solution and we have the following error bounds [26, Sect. 3 and 4]

$$\begin{aligned} \|\mathbf{u}-\mathbf{u}_h\|_h &\leq C\big[\gamma_h^{-1} \inf_{\mathbf{v}\in\mathbf{V}_h} \|\mathbf{u}-\mathbf{v}\|_h + \inf_{q\in Q_h} \|p-q\|_0 + \mathcal{R}_h(\mathbf{u},p)\big], \\ \|p-p_h\|_0 &\leq C\big[\gamma_h^{-1} \inf_{q\in Q_h} \|p-q\|_0 + \gamma_h^{-2} \inf_{\mathbf{v}\in\mathbf{V}_h} \|\mathbf{u}-\mathbf{v}\|_h + \gamma_h^{-1}\mathcal{R}_h(\mathbf{u},p)\big], \end{aligned} \tag{14}$$

where the constants C only depend on α_1, α_2 and β, and where $\mathcal{R}_h(\mathbf{u},p)$ is the residual defined by

$$\mathcal{R}_h(\mathbf{u},p) := \sup_{\mathbf{0}\neq\mathbf{v}\in\mathbf{V}_h} \frac{|A_h(\mathbf{u},\mathbf{v}) + B_h(\mathbf{v},p) - F_h(\mathbf{v})|}{\|\mathbf{v}\|_h}. \tag{15}$$

In [26], the above conditions have been verified on isotropically refined, shape-regular meshes and it has been proved in [26, Theorem 9.1] that, for δ of the order k^2/h, the estimates in (14) are optimal in the mesh sizes and slightly suboptimal in the polynomial degrees. In particular, we point out that the residual $\mathcal{R}_h$ in (15) has been shown to be optimally convergent.

In the following, we generalize these results and show that the forms in (8) satisfy the above conditions on geometric edge meshes, which may be highly anisotropic. In particular, we show that the constants α_1, α_2, β and γ_h can be bounded independently of the aspect ratio of the anisotropic elements in the meshes, for a suitable choice of the discontinuity stabilization parameter δ. Geometric edge meshes are introduced in section 3. Continuity and coercivity properties are then shown in section 4. The crucial stability result is the discrete inf-sup condition in section 5.

3 Geometric edge meshes

In this section, we introduce a class of *geometric meshes* designed to resolve corner and edge singularities that arise in Stokes flow or nearly incompressible elasticity. These meshes are referred to as *geometric edge meshes*; they are, roughly speaking, tensor products of meshes that are geometrically refined towards the edges.

3.1 Construction of geometric edge meshes

Geometric edge meshes are determined by a *mesh grading factor* $\sigma \in (0,1)$ and a *number of layers* n, the thinnest layer having width proportional to σ^n.

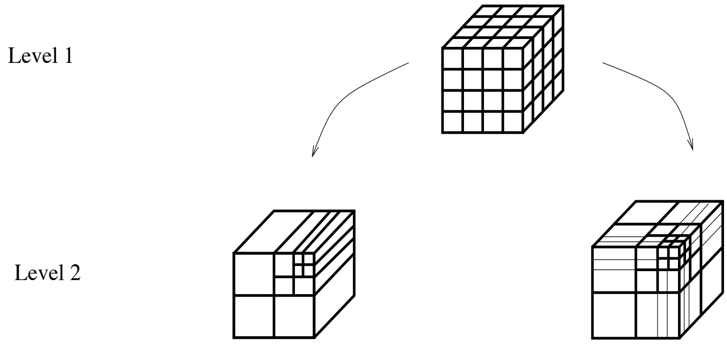

Figure 1: Hierarchic structure of a geometric edge mesh $\mathcal{T}^{n,\sigma}$. The macro-elements M touching the boundary of Ω (level 1) are further refined as edge and corner patches (level 2). Here we have chosen $\sigma = 0.5$ and $n = 3$.

We recall that exponential convergence of *hp*-finite element approximations is achieved if n is suitably chosen. For singularity resolution, n is required to be proportional to the polynomial degree k; see [3, 5].

On Ω, a *geometric edge mesh* $\mathcal{T}^{n,\sigma}$ is constructed by considering an initial shape-regular macro-triangulation $\mathcal{T}_m = \{M\}$ of Ω, possibly consisting of just one element. The macro-elements M in the interior of Ω can be refined isotropically and regularly (not discussed further) while the macro-elements M touching the boundary of Ω are refined geometrically and anisotropically towards edges and corners. This geometric refinement is obtained by affinely mapping reference triangulations (referred to as *patches*) on $\widehat{Q}$ onto the macro-elements M using elemental maps $F_M : \widehat{Q} \to M$. An illustration of this process is shown in Figure 1. For edge meshes, the following patches on $\widehat{Q} = \widehat{I}^3$, $\widehat{I} = (-1, 1)$, are used for the geometric refinement towards the boundary of Ω:

Edge patches: An edge patch $\mathcal{T}_e^{n,\sigma}$ on $\widehat{Q}$ is given by

$$\mathcal{T}_e^{n,\sigma} := \{K_{xy} \times \widehat{I} \mid \quad K_{xy} \in \mathcal{T}_{xy}^{n,\sigma}\},$$

where $\mathcal{T}_{xy}^{n,\sigma}$ is an irregular corner mesh, geometrically refined towards a vertex of $\widehat{S} = \widehat{I}^2$ with grading factor σ and n layers of refinement; see Figure 1 (level 2, left).

Corner patches: In order to build a corner patch $\mathcal{T}_c^{n,\sigma}$ on $\widehat{Q}$, we first consider an initial, irregular, corner mesh $\mathcal{T}_{c,m}^{n,\sigma}$, geometrically refined towards a vertex of $\widehat{Q}$, with grading factor σ and n layers of refinement; see the mesh in bold lines in Figure 1 (level 2, right). The elements of this mesh are then irregularly refined towards the three edges adjacent to the vertex in order to obtain the mesh $\mathcal{T}_c^{n,\sigma}$.

For simplicity, we always assume that the only hanging nodes contained in geometric edge meshes $\mathcal{T}^{n,\sigma}$ are those contained in the edge and corner patches.

The geometric edge meshes satisfy the following property; see also [17].

Property 3.1. *Let $\mathcal{T}^{n,\sigma}$ be a geometric edge mesh on Ω and $K \in \mathcal{T}^{n,\sigma}$. Then K can be written as $K = F_K(K_{xyz})$, where K_{xyz} is of the form*

$$K_{xyz} = I_x \times I_y \times I_z = (x_1, x_2) \times (y_1, y_2) \times (z_1, z_2),$$

and F_K is an affine mapping, the Jacobian of which satisfies

$$|\det(J_K)| \leq C, \qquad |\det(J_K^{-1})| \leq C,$$

with C only depending on the angles of K but not on its dimensions.

We note that the constants in Property 3.1 only depend on the constant in (4) for the underlying macro-element mesh $\mathcal{T}_m$. The dimensions of K_{xyz} on the other hand may depend on the geometric grading factor and the number of refinements.

For an element K of a geometric edge mesh, we define, according to Property 3.1,

$$h_x^K = h_x = x_2 - x_1, \quad h_y^K = h_x = y_2 - y_1, \quad h_z^K = h_x = z_2 - z_1.$$

3.2 Discontinuity stabilization on geometric meshes

In this section, we define the discontinuity stabilization parameter $\delta \in L^\infty(\mathcal{E})$ on geometric edge meshes. Let f be an entire face of an element K of a geometric edge mesh $\mathcal{T}^{n,\sigma}$ on Ω. According to Property 3.1, K can be obtained by a stretched parallelepiped K_{xyz} by an affine mapping F_K that only changes the angles. Suppose that the face f is the image of, e.g., the face $\{x = x_1\}$. We set $h_f = h_x$. For a face perpendicular to the y– or z–direction, we choose $h_f = h_y$ or $h_f = h_z$.

Let now K and K' be two elements with entire faces f and f' that share an interior face, e.g., $f = f \cap f'$ in $\mathcal{E}_\mathcal{I}$. We have

$$c h_f \leq h_{f'} \leq c^{-1} h_f, \tag{16}$$

with a constant $c > 0$ that only depends on the geometric grading factor σ and the constant in (4) for the underlying macro-element mesh $\mathcal{T}_m$. We then define the function $\mathtt{h} \in L^\infty(\mathcal{E})$ by

$$\mathtt{h}(\mathbf{x}) := \begin{cases} \min\{h_f, h_{f'}\} & \mathbf{x} \in f \cap f' \subset \mathcal{E}_\mathcal{I}, \\ h_f & \mathbf{x} \in f \subset \mathcal{E}_\mathcal{B}. \end{cases} \tag{17}$$

Furthermore, we define

$$\delta(\mathbf{x}) = \delta_0 \mathtt{h}^{-1} k^2, \tag{18}$$

with a parameter $\delta_0 > 0$ that is independent of $\mathtt{h}$ and k.

Remark 3.1. *For isotropically refined, shape-regular meshes, the definition in (18) is equivalent to the usual definition of δ, see [26].*

Strongly related to the choice of δ in (17) is the following discrete trace inequality.

Lemma 3.1. *Let K be an element of a geometric edge mesh $\mathcal{T}^{n,\sigma}$ on Ω and f an entire face of K. Then*

$$\|\varphi\|_{0,f}^2 \leq C h_f^{-1} \max\{1,k\}^2 \|\varphi\|_{0,K}^2$$

for any $\varphi \in \mathbb{Q}_k(K)$, $k \geq 0$, with a constant only depending on the constants in Property 3.1.

Proof. First we note that on the reference cube $\widehat{Q}$, this estimate follows from standard inverse inequalities, see, e.g., [27, Theorem 4.76]. Next, let $K = K_{xyz} = (x_1, x_2) \times (y_1, y_2) \times (z_1, z_2)$ be an axiparallel element. We may assume that the face f is given by $f_{yz} = \{x_1\} \times (y_1, y_2) \times (z_1, z_2)$. A simple scaling argument then yields

$$\|\varphi\|_{0,f_{yz}}^2 \leq C h_x^{-1} \max\{1,k\}^2 \|\varphi\|_{0,K_{xyz}}^2 \tag{19}$$

for any $\varphi \in \mathbb{Q}_k(K_{xyz})$, with $h_x = x_2 - x_1$ and an absolute constant $C > 0$. Finally, since an element K of a geometric edge mesh can be written as $K = F_K(K_{xyz})$ according to Property 3.1, the claim follows from (19) by a scaling argument that takes into account the definition of h_f. □

4 Continuity and coercivity on geometric edge meshes

Our first main result establishes the continuity of A_h and B_h as well as the coercivity of A_h on geometric edge meshes.

Theorem 4.1. *Let $\mathcal{T}^{n,\sigma}$ be a geometric edge mesh on Ω with a grading factor $\sigma \in (0,1)$ and n layers of refinement. Let the discontinuity stabilization function δ be defined as in (17) and (18).*

The forms A_h and B_h in (8) are continuous,

$$\begin{aligned} |A_h(\mathbf{v},\mathbf{w})| &\leq \nu\alpha_1 \|\mathbf{v}\|_h \|\mathbf{w}\|_h \qquad && \forall\, \mathbf{v},\mathbf{w} \in \mathbf{V}(h), \\ |B_h(\mathbf{v},q)| &\leq \alpha_2 \|\mathbf{v}\|_h \|q\|_0 && \forall\, \mathbf{u} \in \mathbf{V}(h),\ q \in Q, \end{aligned}$$

with continuity constants α_1 and α_2 that depend on δ_0 and the constants in Property 3.1, but are independent of ν, k, n, and the aspect ratio of the anisotropic elements in $\mathcal{T}^{n,\sigma}$.

Furthermore, there exists a constant $\delta_{\min} > 0$ that depends on the constants in Property 3.1, but is independent of ν, k, n, and the aspect ratio of the anisotropic elements in $\mathcal{T}^{n,\sigma}$, such that, for any $\delta_0 \geq \delta_{\min}$,

$$A_h(\mathbf{v},\mathbf{v}) \geq \nu\beta \|\mathbf{v}\|_h^2 \qquad \forall\, \mathbf{v} \in \mathbf{V}_h,$$

for a coercivity constant $\beta > 0$ depending on δ_0 and the constants in Property 3.1, but independent of ν, k, n, and the aspect ratio of the anisotropic elements in $\mathcal{T}^{n,\sigma}$.

Proof. We first claim that the lifting operators $\underline{\mathcal{L}}$ and $\mathcal{M}$ in (5) and (6) satisfy

$$\|\underline{\mathcal{L}}(\mathbf{v})\|_0^2 \leq C \int_{\mathcal{E}} \delta \, |\underline{[\![\mathbf{v}]\!]}|^2 \, ds, \qquad \|\mathcal{M}(\mathbf{v})\|_0^2 \leq C \int_{\mathcal{E}} \delta \, |\underline{[\![\mathbf{v}]\!]}|^2 \, ds, \tag{20}$$

for all $\mathbf{v} \in \mathbf{V}(h)$, with $C > 0$ independent of k, n, and the aspect ratio of the anisotropic elements.

We show the first estimate in (20) for $\underline{\mathcal{L}}$; the proof of the second estimate is completely analogous by noting that $|[\![\mathbf{v}]\!]|^2 \leq |\underline{[\![\mathbf{v}]\!]}|^2$. For $\mathbf{v} \in \mathbf{V}(h)$, we have

$$\begin{aligned}
\|\underline{\mathcal{L}}(\mathbf{v})\|_0 &= \sup_{\underline{\tau} \in \underline{\Sigma}_h} \frac{\int_\Omega \underline{\mathcal{L}}(\mathbf{v}) : \underline{\tau} \, d\mathbf{x}}{\|\underline{\tau}\|_0} = \sup_{\underline{\tau} \in \underline{\Sigma}_h} \frac{\int_{\mathcal{E}} \underline{[\![\mathbf{v}]\!]} : \{\!\{\underline{\tau}\}\!\} \, ds}{\|\underline{\tau}\|_0} \\
&\leq \sup_{\underline{\tau} \in \underline{\Sigma}_h} \frac{\left(\int_{\mathcal{E}} \delta |\underline{[\![\mathbf{v}]\!]}|^2 \, ds\right)^{\frac{1}{2}} \left(\int_{\mathcal{E}} \delta^{-1} |\{\!\{\underline{\tau}\}\!\}|^2 \, ds\right)^{\frac{1}{2}}}{\|\underline{\tau}\|_0} \\
&\leq C \sup_{\underline{\tau} \in \underline{\Sigma}_h} \frac{\left(\int_{\mathcal{E}} \delta |\underline{[\![\mathbf{v}]\!]}|^2 \, ds\right)^{\frac{1}{2}} \left(\sum_{K \in \mathcal{T}_h} \int_{\partial K} \delta^{-1} |\underline{\tau}|^2 ds\right)^{\frac{1}{2}}}{\|\underline{\tau}\|_0}.
\end{aligned}$$

Here, we used the definition of $\underline{\mathcal{L}}$ and Cauchy-Schwarz inequalities. Since for $\underline{\tau} \in \underline{\Sigma}_h$

$$\int_{\partial K} \delta^{-1} |\underline{\tau}|^2 ds \leq C \sum_{m=1}^{6} h_{f_m} k^{-2} \|\underline{\tau}\|_{0,f_m}^2 \leq C \|\underline{\tau}\|_{0,K},$$

thanks to the definition of δ and Lemma 3.1, we obtain the desired estimate for $\underline{\mathcal{L}}$.

The continuity of the forms A_h and B_h follows immediately from (20) and Cauchy-Schwarz inequalities. The coercivity of A_h can be proven by employing the first estimate in (20) and the arithmetic-geometric mean inequality $2ab \leq \varepsilon a^2 + \varepsilon^{-1} b^2$, for all $\varepsilon > 0$, see [4]. □

Remark 4.1. *The results in Theorem 4.1 are based on the anisotropic stability estimates (20) for the lifting operators $\underline{\mathcal{L}}$ and $\mathcal{M}$. These operators are identical for all the DG forms considered in [26] and, thus, the results in this section holds true for all the mixed DG methods there as well. We also note that the restriction on δ_0 is typical for the interior penalty form A_h and can be avoided if A_h is chosen to be, e.g., the local discontinuous Galerkin form, the nonsymmetric interior penalty form or the second Bassi-Rebay form, see [26].*

5 Divergence stability on geometric edge meshes

Our second main result establishes the divergence stability in (13) for $\mathbb{Q}_k - \mathbb{Q}_{k-1}$ elements on geometric edge meshes. We have the following theorem.

Theorem 5.1. *Let $\mathcal{T}^{n,\sigma}$ be a geometric edge mesh on Ω with a grading factor $\sigma \in (0, 1)$ and n layers of refinement. Let the discontinuity stabilization function*

δ be defined as in (17) and (18). Then there exists a constant $C > 0$ that depends on σ and the shape-regularity of the macro-element mesh, but is independent of k, n, and the aspect ratio of the anisotropic elements in $\mathcal{T}^{n,\sigma}$, such that, for any n and $k \geq 2$,

$$\inf_{0 \neq q \in Q_h^{k-1}(\mathcal{T}^{n,\sigma})} \sup_{0 \neq \mathbf{v} \in \mathbf{V}_h^k(\mathcal{T}^{n,\sigma})} \frac{B_h(\mathbf{v}, q)}{\|\mathbf{v}\|_h \, \|q\|_0} \geq C k^{-3/2}.$$

Hence, condition (13) is satisfied with $\gamma_h = C k^{-3/2}$.

Remark 5.1. *This result extends the work in [24, 25, 33] for conforming $\mathbb{Q}_k - \mathbb{Q}_{k-2}$ elements to the discontinuous Galerkin context; it is proved in a similar way using a macro-element technique. We point out, however, that in the DG approximations considered here we use $\mathbb{Q}_k - \mathbb{Q}_{k-1}$ elements that are unstable in a conforming setting. This choice of spaces is optimal from an approximation point of view.*

Remark 5.2. *The form B_h is identical for the DG methods in [13, 20, 32, 26]. Therefore, the stability result in Theorem 5.1 is valid for all these methods.*

The proof of Theorem 5.1 is carried out in the remaining sections. The first ingredient we need is a macro-element technique that we introduce in section 6. The second ingredient is given by some stability estimates for Raviart-Thomas interpolants on certain anisotropic meshes, derived in section 7. In section 8, we establish divergence stability on edge patches. The proof of Theorem 5.1 is completed in section 9 by recursively applying the macro-element technique.

6 Macro-element technique

In order to prove Theorem 5.1, we use a macro-element technique; see [30, 31, 25, 33]. We recall that a geometric edge mesh $\mathcal{T} = \mathcal{T}^{n,\sigma}$ is obtained by refining a coarser, shape-regular macro-mesh $\mathcal{T}_m$. Theorem 6.1 below is the main tool of our macro-element technique.

First, we introduce local bilinear forms. If $M \in \mathcal{T}_m$, we define

$$B_{h,M}(\mathbf{v}, q) = -\int_M q \, \nabla_h \cdot \mathbf{v} \, d\mathbf{x} + \int_{\mathcal{E}_\mathcal{I} \cap M} \{\!\{q\}\!\} [\![\mathbf{v}]\!] \, ds + \int_{\mathcal{E} \cap \partial M} q \, \mathbf{v} \cdot \mathbf{n} \, ds, \quad (21)$$

for $(\mathbf{v}, q) \in \mathbf{V}_h^k(\mathcal{T}) \times Q_h^{k-1}(\mathcal{T})$. Correspondingly, we also need the local norm

$$\|\mathbf{v}\|_{h,M}^2 = \sum_{\substack{K \in \mathcal{T} \\ K \subset M}} |\mathbf{v}|_{1,K}^2 + \int_{\mathcal{E}_\mathcal{I} \cap M} \delta_M |\underline{[\![\mathbf{v}]\!]}|^2 \, ds + \int_{\mathcal{E} \cap \partial M} \delta_M |\mathbf{v} \otimes \mathbf{n}_M|^2 \, ds, \quad (22)$$

where $\mathbf{n}_M$ denotes the outward normal unit vector to ∂M and δ_M is a discontinuity stabilization function defined as in (18), with $\mathtt{h}(\mathbf{x})$ replaced by

$$\mathtt{h}_M(\mathbf{x}) := \begin{cases} \mathtt{h}(\mathbf{x}) & \mathbf{x} \in f \subset \mathcal{E}_\mathcal{I} \setminus \partial M, \\ h_f & \mathbf{x} \in f \subset \partial M. \end{cases} \quad (23)$$

By integration by parts on each element in M, we have

$$B_{h,M}(\mathbf{v},q) = \int_M \mathbf{v}\cdot\nabla_h q\,d\mathbf{x} - \int_{\mathcal{E}_\mathcal{I}\cap M} [\![q]\!]\cdot\{\!\{\mathbf{u}\}\!\}\,ds. \tag{24}$$

If $\mathcal{T}_M$ is the restriction of $\mathcal{T}$ to M, then

$$B_{h,M}(\mathbf{v},q) = B_h(\mathbf{v},q), \qquad \mathbf{v}\in\widetilde{\mathbf{V}}_h^k(\mathcal{T}_M;M), \tag{25}$$

where we use the same notation for $\mathbf{v}\in\widetilde{\mathbf{V}}_h^k(\mathcal{T}_M;M)$ and its extension by zero to Ω.

For a geometric edge mesh on Ω, we have

$$\delta(\mathbf{x}) \le c\delta_M(\mathbf{x}), \qquad \delta(\mathbf{x}) \le c\delta_{M'}(\mathbf{x}), \qquad \mathbf{x}\in\partial M\cap\partial M', \tag{26}$$

with $c>0$ solely depending on σ and the shape-regularity of the macro-element mesh $\mathcal{T}_m$. This follows from the construction of geometric edge meshes, from the definition of δ in (17), (18), and from (16).

The following theorem holds.

Theorem 6.1. *Let $\mathcal{T}=\mathcal{T}^{n,\sigma}$ be a geometric edge mesh on Ω with a grading factor $\sigma\in(0,1)$ and n layers of refinement. Let $\mathcal{T}_m$ be the underlying macro-element mesh. Assume that there exists a low-order space $\mathbf{X}_h\subseteq\mathbf{V}_h^k(\mathcal{T})$ such that*

$$\inf_{0\neq q\in Q_h^0(\mathcal{T}_m)}\ \sup_{0\neq\mathbf{v}\in\mathbf{X}_h}\frac{B_h(\mathbf{v},q)}{\|\mathbf{v}\|_h\,\|q\|_0}\ge C_1, \tag{27}$$

with a constant $C_1>0$ independent of k. Furthermore, assume that there exists a constant $C_2>0$ independent of $M\in\mathcal{T}_m$ and k such that

$$\inf_{0\neq q\in Q_h^{k-1}(\mathcal{T}_M;M)}\ \sup_{0\neq\mathbf{v}\in\widetilde{\mathbf{V}}_h^k(\mathcal{T}_M;M)}\frac{B_{h,M}(\mathbf{v},q)}{\|v\|_{h,M}\|q\|_{0,M}}\ge C_2\,k^{-\alpha}, \qquad M\in\mathcal{T}_m, \tag{28}$$

with $\alpha\ge 0$ and $\mathcal{T}_M$ denoting the restriction of $\mathcal{T}$ to $M\in\mathcal{T}_m$. Then the spaces $\mathbf{V}_h^k(\mathcal{T})$ and $Q_h^{k-1}(\mathcal{T})$ satisfy

$$\inf_{0\neq q\in Q_h^{k-1}(\mathcal{T})}\ \sup_{0\neq\mathbf{v}\in\mathbf{V}_h^k(\mathcal{T})}\frac{B_h(\mathbf{v},q)}{\|\mathbf{v}\|_h\,\|q\|_0}\ge Ck^{-\alpha},$$

with a constant $C>0$ solely depending on C_1, C_2, σ and the shape-regularity of $\mathcal{T}_m$.

Proof. Let $q\in Q_h^{k-1}(\mathcal{T})$. We decompose q into $q=q^*+q_m$ where q_m is the $L^2(\Omega)$-projection of q onto the space $Q_h^0(\mathcal{T}_m)$ of piecewise constant pressures on the macro-element mesh $\mathcal{T}_m$. Because of (27), there exists $\mathbf{v}_m\in\mathbf{X}_h$ such that

$$B_h(\mathbf{v}_m,q_m)\ge\|q_m\|_0^2, \qquad \|\mathbf{v}_m\|_h\le C_1^{-1}\|q_m\|_0. \tag{29}$$

We next consider $q^* \in Q_h^{k-1}(\mathcal{T})$. We fix a macro-element $M \in \mathcal{T}_m$ and set $q_M^* := q^*|_M$. We note that q_M^* has vanishing mean value on M. By using (28), there exists a field $\mathbf{v}_M^*$ in $\widetilde{\mathbf{V}}_h^k(\mathcal{T}_M; M)$ such that

$$B_{h,M}(\mathbf{v}_M^*, q_M^*) \geq \|q_M^*\|_{0,M}^2, \qquad \|\mathbf{v}_M^*\|_{h,M} \leq C_2^{-1} k^\alpha \|q_M^*\|_{0,M}. \tag{30}$$

We now define $\mathbf{v}^* = \sum_{M \in \mathcal{T}_m} \mathbf{v}_M^*$. By construction, $\mathbf{v}_M^*$ has a vanishing normal component on ∂M and vanishes outside M. Thus, combining (25) with (30) yields

$$B_h(\mathbf{v}^*, q^*) = \sum_{M \in \mathcal{T}_m} B_{h,M}(\mathbf{v}_M^*, q_M^*) \geq \|q^*\|_0^2. \tag{31}$$

Furthermore, thanks to (26) and (30),

$$\|\mathbf{v}^*\|_h^2 \leq C \sum_{M \in \mathcal{T}_m} \|\mathbf{v}_M^*\|_{h,M}^2 \leq C k^{2\alpha} \|q^*\|_0^2, \tag{32}$$

with a constant C only depending on C_2 and the constant in (26). Select now $\mathbf{v} = \mathbf{v}_m + \eta \mathbf{v}^* \in \mathbf{V}_h^k(\mathcal{T})$ where $\eta > 0$ is still at our disposal. First, thanks to (25), (24) and the fact that q_m is constant on each macro-element, we have

$$\begin{aligned} B_h(\mathbf{v}^*, q_m) &= \sum_{M \in \mathcal{T}_m} B_{h,M}(\mathbf{v}_M^*, q_m) \\ &= \sum_{M \in \mathcal{T}_m} \left(\int_M \mathbf{v}_M^* \cdot \nabla_h q_m \, d\mathbf{x} - \int_{\mathcal{E}_\mathcal{I} \cap M} [\![q_m]\!] \cdot \{\!\{ \mathbf{v}_M^* \}\!\} \, ds \right) = 0. \end{aligned}$$

Further, the continuity of $B_h(\cdot, \cdot)$ in Theorem 4.1, (29), and the arithmetic-geometric mean inequality yield

$$|B_h(\mathbf{v}_m, q^*)| \leq \alpha_2 \|\mathbf{v}_m\|_h \|q^*\|_0 \leq C \|q_m\|_0 \|q^*\|_0 \leq \frac{C}{\varepsilon} \|q_m\|_0^2 + \varepsilon C \|q^*\|_0^2,$$

with another parameter $\varepsilon > 0$ to be properly chosen. Combining the above results with (29) and (31), gives

$$\begin{aligned} B_h(\mathbf{v}, q) &= B_h(\mathbf{v}_m, q_m) + B_h(\mathbf{v}_m, q^*) + \eta B_h(\mathbf{v}^*, q^*) \\ &\geq (1 - \frac{C}{\varepsilon}) \|q_m\|_0^2 + (\eta - \varepsilon C) \|q^*\|_0^2. \end{aligned}$$

It then clear that we can choose η and ε in such a way that

$$B_h(\mathbf{v}, q) \geq c \|q\|_0^2 \tag{33}$$

with a constant c independent of k. Furthermore, from (29) and (32),

$$\|\mathbf{v}\|_h \leq \|\mathbf{v}_m\|_h + \eta \|\mathbf{v}^*\|_h \leq c k^\alpha \|q\|_0. \tag{34}$$

The assertion of Theorem 6.1 follows then from (33) and (34). $\square$

For geometric edge meshes, the macro-elements are refined by mapping reference configurations on $\widehat{Q}$. Condition (28) in Theorem 6.1 can then be verified by checking the stability of the patches on the reference cube $\widehat{Q}$. Similarly to (21) and (22), we denote by $B_{h,\widehat{Q}}(\cdot,\cdot)$ and $\|\cdot\|_{h,\widehat{Q}}$ the divergence form and the broken energy norm on a mesh on $\widehat{Q}$, respectively, with the stabilization function $\delta_{\widehat{Q}}$ defined according to (18), but with $\mathtt{h}$ replaced by the local mesh-size $\mathtt{h}_{\widehat{Q}}$ defined as in (23) with $M = \widehat{Q}$.

Proposition 6.1. *Let $\mathcal{T} = \mathcal{T}^{n,\sigma}$ be a geometric edge mesh on Ω with a grading factor $\sigma \in (0,1)$ and n layers of refinement. Let $\mathcal{T}_m$ be the underlying macro-element mesh, and $\mathcal{F}$ be a family of meshes on the reference element $\widehat{Q}$, also containing the trivial triangulation $\widehat{\mathcal{T}} = \{\widehat{Q}\}$. Assume that $\mathcal{T}$ is obtained from $\mathcal{T}_m$ by further partitioning the elements of $\mathcal{T}_m$ into $F_M(\widehat{\mathcal{T}})$ where $\widehat{\mathcal{T}} \in \mathcal{F}$ and F_M is the affine mapping between $\widehat{Q}$ and M. Assume that the family $\mathcal{F}$ is uniformly stable in the sense that*

$$\inf_{0\neq q\in Q_h^{k-1}(\widehat{\mathcal{T}};\widehat{Q})} \sup_{0\neq \mathbf{v}\in \widetilde{\mathbf{V}}_h^k(\widehat{\mathcal{T}};\widehat{Q})} \frac{B_{h,\widehat{Q}}(\mathbf{v},q)}{\|v\|_{h,\widehat{Q}}\|q\|_{0,\widehat{Q}}} \geq C\,k^{-\alpha}, \qquad \forall \widehat{\mathcal{T}} \in \mathcal{F},\ \forall k, \tag{35}$$

with a constant $C > 0$ independent of $\widehat{\mathcal{T}} \in \mathcal{F}$ and k. Then, condition (28) in Theorem 6.1 is satisfied with a constant that only depends on the constant in (35) and the shape-regularity of the macro-element mesh $\mathcal{T}_m$.

Proof. Let $M \in \mathcal{T}_m$ be a macro-element. The restriction $\mathcal{T}_M$ of $\mathcal{T}$ to M is given by $F_M(\widehat{\mathcal{T}})$ for some mesh $\widehat{\mathcal{T}} \in \mathcal{F}$. Let $q \in Q_h^{k-1}(\mathcal{T}_M; M)$. We transform q back to the reference element $\widehat{Q}$ via the affine transformation $F_M : \widehat{Q} \to M$, that is, we set $\widehat{q} = q \circ F_M \in Q_h^{k-1}(\widehat{\mathcal{T}}; \widehat{Q})$. By (35), there exists $\widehat{\mathbf{v}} \in \widetilde{\mathbf{V}}_h^k(\widehat{\mathcal{T}}; \widehat{Q})$ such that

$$B_{h,\widehat{Q}}(\widehat{\mathbf{v}},\widehat{q}) \geq \|\widehat{q}\|_{0,\widehat{Q}}^2, \qquad \|\widehat{\mathbf{v}}\|_{h,\widehat{Q}} \leq C^{-1}k^{\alpha}\|\widehat{q}\|_{0,\widehat{Q}}. \tag{36}$$

We use the Piola-transform, see [9, Sect. III.1], and set

$$\mathbf{v} = P_M(\widehat{\mathbf{v}}) = |J_M|^{-1} J_M \widehat{\mathbf{v}} \circ F_M^{-1}.$$

Here, J_M is the Jacobian of F_M and $|J_M| = |\det(J_M)|$. Let now $K = F_M(\overline{K})$ be an element of M that is the image of the element $\overline{K}$ in $\widehat{Q}$. It can then be easily seen that $\mathbf{v}|_K$ is obtained from $\widehat{\mathbf{v}}|_{\overline{K}}$ through the local Piola transformation $\overline{K} \to K$. Due to the properties of these transforms in [9, Lemma 1.5 and Lemma 1.6], we thus have $\mathbf{v} \in \widetilde{\mathbf{V}}_h^k(\mathcal{T}_M; M)$ and $B_{h,\widehat{Q}}(\widehat{\mathbf{v}},\widehat{q}) = B_{h,M}(\mathbf{v},q)$. By using the definition of δ_M and $\delta_{\widehat{Q}}$ and standard scaling properties for the Piola-transform, we obtain from (36) the existence of a field in $\widetilde{\mathbf{V}}_h^k(\mathcal{T}_M; M)$ also denoted by $\mathbf{v}$ such that

$$B_{h,M}(\mathbf{v},q) \geq \|q\|_{0,M}^2, \qquad \|\mathbf{v}\|_{h,M} \leq Ck^{\alpha}\|q\|_{0,M},$$

where C solely depends on the constant in (35) and the shape-regularity of the macro-element mesh $\mathcal{T}_m$. □

7 Raviart-Thomas interpolant on anisotropic meshes

The purpose of this section is to provide estimates for the interpolant on Raviart-Thomas finite element spaces on certain anisotropic meshes. In order to do so, we employ a different representation than that considered in [26], originally proposed in [2].

7.1 One-dimensional interpolants

We first introduce some one-dimensional projections. Let $\{L_i(x),\ i \in \mathbb{N}_0\}$ be the set of orthogonal Legendre polynomials on $\hat{I} = (-1, 1)$; see, e.g., [7]. We also consider a different set $\{U_i(x),\ i \in \mathbb{N}_0\}$

$$\begin{aligned} &U_0(x) = L_0(x) = 1, \qquad U_1(x) = L_1(x) = x, \\ &U_i(x) = \int_{-1}^{x} L_{i-1}(t)dt = (2i-1)^{-1}(L_i - L_{i-2}), \quad i \geq 2; \end{aligned} \tag{37}$$

see in particular [7, Theorem 3.3]. The sets $\{L_i\}$ and $\{U_i\}$ both provide bases for $L^2(\hat{I})$ and thus $H^1(\hat{I})$.

For a generic interval $I = (x_1, x_2) = F_I(\hat{I})$, two bases can be found by mapping $\{L_i\}$ and $\{U_i\}$ onto I. In the following, we use the same notations for these bases in $L^2(I)$ as for the reference interval.

Let $\pi_k^0 : L^2(I) \to \mathbb{Q}_k(I)$ be the L^2-orthogonal projection. We note that

$$\pi_k^0\left(\sum_{i=0}^{\infty} v_i L_i\right) = \sum_{i=0}^{k} v_i L_i.$$

We also define a second projection $\pi_k^1 : L^2(I) \to \mathbb{Q}_k(I)$ by

$$\pi_k^1\left(\sum_{i=0}^{\infty} \widetilde{v}_i U_i\right) = \sum_{i=0}^{k} \widetilde{v}_i U_i.$$

Lemma 7.1. *Let $I = (x_1, x_2)$. For $v \in H^1(I)$, we have*

$$\begin{aligned} &(\pi_k^1 v)(x_1) = v(x_1), \qquad (\pi_k^1 v)(x_2) = v(x_2), \qquad k \geq 1, \\ &\int_I \pi_k^1 v q\, dx = \int_I vq\, dx \quad q \in \mathbb{Q}_{k-2}(I), \qquad k \geq 2. \end{aligned}$$

Proof. The first property follows from the fact that $U_i(x_1) = U_i(x_2) = 0$ for $i \geq 2$. To prove the second property, let $q \in \mathbb{Q}_{k-2}(I)$ be given by $q = L'_{i-1}$ for $2 \leq i \leq k$. It is then easy to see that

$$\int_I (\pi_k^1 v)' L_{i-1} dx = \int_I v' L_{i-1} dx.$$

From the above identity and the first assertion, the second assertion follows by integration by parts. $\square$

The next lemma provides certain stability estimates.

Lemma 7.2. *Let $I = (x_1, x_2)$ and $v \in H^1(I)$. There is a constant $C > 0$ independent of k and I such that*

$$\|\pi_k^0 v\|_{0,I} \le \|v\|_{0,I}, \qquad |\pi_k^0 v|_{1,I} \le C\sqrt{k}\,|v|_{1,I}, \qquad |\pi_k^1 v|_{1,I} \le |v|_{1,I}.$$

If in addition $v \in H_0^1(I)$, then

$$\|\pi_k^1 v\|_{0,I} \le C\sqrt{k}\,\|v\|_{0,I}. \tag{38}$$

Proof. Since for a generic interval the bounds are obtained by a standard scaling argument, it is enough to consider $I = (-1, 1)$. The bounds for π_k^0 can be found in [10]. Moreover, let $v = \sum_{i=0}^{\infty} v_i U_i$ and $\chi : [0, \infty) \to \mathbb{R}$ be a C^1 cut-off function that is equal to one in $[0, 1]$, decreases to zero in $[1, 1 + \mu]$, and is equal to zero in $[1 + \mu, \infty)$. If $\mu = 1/k$, it is easy to prove that $\pi_k^1 v = \sum_{i=0}^{\infty} \chi\left(\frac{i}{k}\right) v_i U_i$. The bounds for π_k^1 can then be found in Lemma 3.2, Lemma 3.3, and Remark 3.4 in [8]. □

Further, we will make use of the following approximation property. It is proved in [21] for the reference interval and can be proved for a generic interval by a scaling argument.

Lemma 7.3. *Let $I = (x_1, x_2)$ and $h = x_2 - x_1$. Then there is a constant $C > 0$ independent of k and I such that for $v \in H^1(I)$*

$$|(\pi_k^0 v - v)(x_i)|^2 \le C\frac{h}{k}|v|_{1,I}^2, \quad i = 1, 2.$$

7.2 Two-dimensional interpolants

We recall some two-dimensional results that were proven in [2, 26]. Given the reference square $\widehat{S}$ and an integer $k \ge 0$, we consider the Raviart-Thomas space

$$RT_k(\widehat{S}) = \mathbb{Q}_{k+1,k}(\widehat{S}) \times \mathbb{Q}_{k,k+1}(\widehat{S}),$$

where $\mathbb{Q}_{k_1,k_2}(\widehat{S})$ is the space of polynomials of degree k_i in the i-th variable on $\widehat{S}$. For an affinely mapped element $K = F_K(\widehat{S})$, the Raviart-Thomas space $RT_k(K)$ is defined by suitably mapping functions in $RT_k(\widehat{S})$ using a Piola transformation; see [9, Sect. 3.3] or [2, Sect. 3.3] for further details.

On $\widehat{S}$, there is a unique interpolation operator $\Pi_{\widehat{S}} = \Pi_{\widehat{S}}^k : H^1(\widehat{S})^2 \to RT_k(\widehat{S})$, such that

$$\begin{aligned} &\int_{\widehat{S}} (\Pi_{\widehat{S}}\mathbf{v} - \mathbf{v}) \cdot \mathbf{w}\, d\mathbf{x} = 0, \qquad \forall \mathbf{w} \in \mathbb{Q}_{k-1,k}(\widehat{S}) \times \mathbb{Q}_{k,k-1}(\widehat{S}),\\ &\int_{\widehat{f}_m} (\Pi_{\widehat{S}}\mathbf{v} - \mathbf{v}) \cdot \mathbf{n}\, \varphi\, ds = 0, \qquad \forall \varphi \in \mathbb{Q}_k(\widehat{f}_m), \quad m = 1, \dots, 4; \end{aligned} \tag{39}$$

see [9] or [2]. For $k = 0$, the first condition in (39) is void. For an affinely mapped element K, the interpolant $\Pi_K = \Pi_K^k : H^1(K)^2 \to RT_k(K)$ can be defined by using a Piola transform in such a way that the orthogonality conditions in (39) also hold for Π_K.

For shape-regular elements, we recall the following result from [26, Lemma 6.9 and Lemma 6.10].

Lemma 7.4. *Let K be a shape-regular element of diameter h_K and $\mathbf{w} \in H^1(K)^3$. Then*

$$|\Pi_K \mathbf{w}|_{1,K} \leq C\, k\, |\mathbf{w}|_{1,K}, \qquad \|\mathbf{w} - \Pi_K \mathbf{w}\|_{0,\partial K}^2 \leq C h_K |\mathbf{w}|_{1,K}^2,$$

with a constant $C > 0$ that is independent of k and h_K.

In addition to the bounds in Lemma 7.4, we need slightly refined estimates to treat axiparallel elements of the form $S = S_{xy} = (x_1, x_2) \times (y_1, y_2)$. Such bounds can be obtained by using tensor product arguments. For this purpose, we define the two-dimensional operators

$$\Pi_k^x := \pi_k^{0,y} \circ \pi_{k+1}^{1,x}, \qquad \Pi_k^y := \pi_{k+1}^{1,y} \circ \pi_k^{0,x},$$

with the one-dimensional projectors π_k^0 and π_k^1 from section 7.1. We have specified the variable on which these projections act.

We have the following representation result.

Lemma 7.5. *The Raviart-Thomas interpolant on $S = S_{xy} = (x_1, x_2) \times (y_1, y_2)$ satisfies*

$$\Pi_S^k \mathbf{v} = \Pi_S^k(v_x, v_y) = (\Pi_k^x v_x, \Pi_k^y v_y), \qquad \mathbf{v} \in C^\infty(\overline{S})^2.$$

Proof. Using Lemma 7.1 and properties of the L^2-projection, it is immediate to see that $(\Pi_k^x v_x, \Pi_k^y v_y)$ satisfies the conditions in (39) on S. □

The operators Π_k^x and Π_k^y can be uniquely extended by density to functions in $H^1(S)$ (these extensions being still denoted by Π_k^x and Π_k^y). This is a consequence of the following result.

Lemma 7.6. *Let $v \in C^\infty(\overline{\widehat{S}})$. Then there exists a constant C independent of k, such that*

$$\|\partial_x(\Pi_k^x v)\|_{0,\widehat{S}} \leq \|\partial_x v\|_{0,\widehat{S}}, \qquad \|\partial_y(\Pi_k^x v)\|_{0,\widehat{S}} \leq Ck\, |v|_{1,\widehat{S}}.$$

Similar estimates hold for Π_k^y.

Proof. The first bound can be proven using the definition of Π_k^x and Π_k^y and the one-dimensional bounds in Lemma 7.2. The second bound can be found in [26, Lemma 6.9]. □

We end this section with an error estimate for the two-dimensional L^2-projection. It can be proven by using Lemma 7.3; cf. [21, Lemma 3.9].

Lemma 7.7. *Let $S = S_{xy} = (x_1, x_2) \times (y_1, y_2)$ be a shape-regular element of diameter h. Then there exists a constant $C > 0$ independent of k and h such that*

$$\|v - \pi_k^{0,y}\pi_k^{0,x}v\|_{0,\partial S}^2 \leq C\frac{h}{k}|v|_{1,S}^2, \qquad v \in H^1(S).$$

7.3 Three-dimensional interpolants

In this section, we introduce the Raviart-Thomas interpolant in three dimensions. We note that we use the same notations as for the two-dimensional case. Given an axiparallel element of the form

$$K_{xyz} = (x_1, x_2) \times (y_1, y_2) \times (z_1, z_2),$$

and an integer $k \geq 0$, we consider the Raviart-Thomas space

$$RT_k(K_{xyz}) = \mathbb{Q}_{k+1,k,k}(K_{xyz}) \times \mathbb{Q}_{k,k+1,k}(K_{xyz}) \times \mathbb{Q}_{k,k,k+1}(K_{xyz}),$$

where $\mathbb{Q}_{k_1,k_2,k_3}(K_{xyz})$ is the space of polynomials of degree k_i in the i-th variable on K_{xyz}. For general affinely mapped elements $K \in \mathcal{T}$ of a geometric edge mesh $\mathcal{T} = \mathcal{T}^{n,\sigma}$ (see Property 3.1), the Raviart-Thomas space $RT_k(K)$ is defined by suitably mapping functions in $RT_k(K_{xyz})$ using a Piola transformation; see [9, Sect. 3.3] or [2, Sect. 3.3] for further details.

On K_{xyz}, there is a unique interpolation operator $\Pi_{K_{xyz}} = \Pi^k_{K_{xyz}} : H^1(K_{xyz})^3 \to RT_k(K_{xyz})$, such that

$$\begin{aligned}
&\int_{K_{xyz}} \big(\Pi_{K_{xyz}}\mathbf{v} - \mathbf{v}\big) \cdot \mathbf{w}\, d\mathbf{x} = 0, \\
&\qquad\qquad \forall \mathbf{w} \in \mathbb{Q}_{k-1,k,k}(K_{xyz}) \times \mathbb{Q}_{k,k-1,k}(K_{xyz}) \times \mathbb{Q}_{k,k,k-1}(K_{xyz}), \\
&\int_{f_m} \big(\Pi_{K_{xyz}}\mathbf{v} - \mathbf{v}\big) \cdot \mathbf{n}\, \varphi\, ds = 0, \quad \forall \varphi \in \mathbb{Q}_{k,k}(f_m), \quad m = 1, \dots, 6;
\end{aligned} \tag{40}$$

with $\{f_m\}$ denoting denoting the six faces of K_{xyz}; see [9] or [2]. For $k = 0$, the first condition in (40) is void. For an element $K \in \mathcal{T}$, the interpolant $\Pi_K = \Pi_K^k : H^1(K)^3 \to RT_k(K)$ can be defined by using a Piola transform in such a way that the orthogonality conditions in (40) also hold for Π_K.

We now define the three-dimensional operators on $K = K_{xyz}$

$$\Pi_k^x := \pi_k^{0,z} \circ \pi_k^{0,y} \circ \pi_{k+1}^{1,x}, \qquad \Pi_k^y := \pi_k^{0,z} \circ \pi_{k+1}^{1,y} \circ \pi_k^{0,x}, \qquad \Pi_k^z := \pi_{k+1}^{1,z} \circ \pi_k^{0,y} \circ \pi_k^{0,x},$$

where we have specified the variable on which the one-dimensional projections act. The following representation result can be proven in the same way as in two dimensions.

Lemma 7.8. *On $K = K_{xyz}$, the Raviart-Thomas interpolant satisfies*

$$\Pi_K^k \mathbf{v} = \Pi_K^k(v_x, v_y, v_z) = (\Pi_k^x v_x, \Pi_k^y v_y, \Pi_k^z v_z), \quad \mathbf{v} \in C^\infty(\overline{K}).$$

The operators Π_k^x, Π_k^y, and Π_k^z are well-defined for functions in $C^\infty(\overline{K})$ and can be uniquely extended by density to $H^1(K)$ (these extensions being still denoted by Π_k^x, Π_k^y and Π_k^z). This is a consequence of the following result.

Lemma 7.9. *Let $v \in C^\infty(\overline{\widehat{Q}})$. Then there exists a constant C independent of k such that*

$$\begin{aligned}
\|\partial_x(\Pi_k^x v)\|_{0,\widehat{Q}}^2 &\leq C\|\partial_x v\|_{0,\widehat{Q}}^2, \\
\|\partial_y(\Pi_k^x v)\|_{0,\widehat{Q}}^2 &\leq Ck^2\,(\|\partial_y v\|_{0,\widehat{Q}}^2 + \|\partial_x v\|_{0,\widehat{Q}}^2), \\
\|\partial_z(\Pi_k^x v)\|_{0,\widehat{Q}}^2 &\leq Ck^2\,(\|\partial_z v\|_{0,\widehat{Q}}^2 + \|\partial_x v\|_{0,\widehat{Q}}^2).
\end{aligned}$$

Similar estimates hold for Π_k^y and Π_k^z.

Proof. The first two estimates can be obtained using Lemmas 7.2 and 7.6, and the fact that Π_k^x can be written as the tensor product of the two-dimensional Raviart-Thomas projection and a one-dimensional L^2-projection: $\Pi_k^x = \pi_k^{0,z} \circ (\pi_k^{0,y} \circ \pi_k^{1,x})$; see Lemma 7.8. The last bound can be obtained by exchanging the y and z variables. □

7.4 Stretched elements

For a general anisotropic element, Lemma 7.9 and a scaling argument provide estimates that are not independent of the aspect ratio. For an edge patch on $\widehat{Q}$, however, we only need to consider stretched elements of the form

$$K_{xyz} = (x_1, x_2) \times (y_1, y_2) \times \widehat{I}, \tag{41}$$

with $h_x = x_2 - x_1 < 2$, $h_y = y_2 - y_1 < 2$, and h_x comparable to h_y. Even for this simpler case, good bounds cannot be found for all the components. However, if we only consider vectors with a vanishing normal component along the faces $z = \pm 1$, we have the following result.

Lemma 7.10. *Let K be given by (41) and $\mathbf{v} = (v_x, v_y, v_z) \in H^1(K)^3$, such that $\mathbf{v} \cdot \mathbf{n}_\pm = 0$ along $z = \pm 1$, with $\mathbf{n}_\pm = (0, 0, \pm 1)$. If $ch_x \leq h_y \leq Ch_x$, then there exists a constant independent of k and the aspect ratio of K, such that*

$$\begin{aligned}
\|\partial_x(\Pi_k^x v_x)\|_{0,K}^2 &\leq C\|\partial_x v_x\|_{0,K}^2, \\
\|\partial_y(\Pi_k^x v_x)\|_{0,K}^2 &\leq Ck^2\,(\|\partial_y v_x\|_{0,K}^2 + \|\partial_x v_x\|_{0,K}^2), \\
\|\partial_z(\Pi_k^x v_x)\|_{0,K}^2 &\leq Ck^2\,(\|\partial_z v_x\|_{0,K}^2 + \|\partial_x v_x\|_{0,K}^2),
\end{aligned}$$

and similarly for $\Pi_k^y v_y$. In addition,

$$\begin{aligned}
\|\partial_x(\Pi_k^z v_z)\|_{0,K}^2 &\leq Ck^2\|\partial_x v_z\|_{0,K}^2, \\
\|\partial_y(\Pi_k^z v_z)\|_{0,K}^2 &\leq Ck^2\|\partial_y v_z\|_{0,K}^2, \\
\|\partial_z(\Pi_k^z v_z)\|_{0,K}^2 &\leq C\|\partial_z v_z\|_{0,K}^2.
\end{aligned}$$

Consequently, $|\Pi_K \mathbf{v}|_{1,K} \leq C\,k\,|\mathbf{v}|_{1,K}$, with a constant independent of k and the aspect ratio of K.

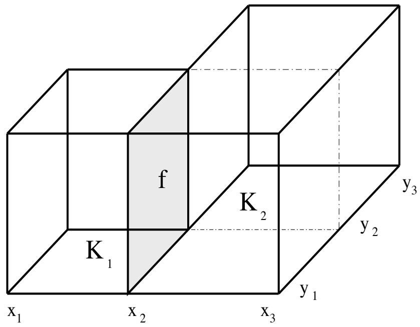

Figure 2: Two stretched elements K_1 and K_2 that share the face $f = \{x_2\} \times (y_1, y_2) \times \widehat{I}$.

Proof. Assume first that $\mathbf{v} \in C^\infty(\overline{K})^3$. The bounds for $\Pi_k^x v_x$ and $\Pi_k^y v_y$ follow from Lemma 7.9 and a scaling argument. To obtain the estimates of $\Pi_k^z v_z$, we use the representation in Lemma 7.8 and the results in Lemma 7.2. In particular, we use (38) to bound $\pi_{k+1}^{1,z}$. The proof is then completed by a density argument. $\square$

Similarly, it is possible to bound the jumps across faces of stretched elements. Let K_1 and K_2 be two stretched elements given by

$$K_1 = (x_1, x_2) \times (y_1, y_2) \times \widehat{I}, \qquad K_2 = (x_2, x_3) \times (y_1, y_3) \times \widehat{I}, \tag{42}$$

with $y_2 \leq y_3$. Further, we introduce the faces $f_1 = \{x_2\} \times (y_1, y_2) \times \widehat{I}$ and $f_2 = \{x_2\} \times (y_1, y_3) \times \widehat{I}$. Let $f = f_1 \subseteq f_2$, as illustrated in Figure 2. We then set $h_{1,x} = x_2 - x_1$, $h_{2,x} = x_3 - x_2$, $h_{1,y} = y_2 - y_1$, and $h_{2,y} = y_3 - y_1$.

Lemma 7.11. *Let K_1 and K_2 be the two stretched elements in (42). Let $\mathbf{u} \in H^1(K_1 \cup K_2)^3$ such that $\mathbf{u} \cdot \mathbf{n}_\pm = 0$ along $z = \pm 1$, with $\mathbf{n}_\pm = (0, 0, \pm 1)$. Assume that*

$$c h_{1,x} \leq h_{2,x} \leq C h_{1,x}, \qquad h_{1,y} \leq h_{2,y} \leq C h_{2,x}.$$

Let $\mathbf{v}$ be the piecewise polynomial given by $\mathbf{v}|_{K_i} = \Pi_{K_i}(\mathbf{u}|_{K_i})$ where Π_{K_i} is the Raviart-Thomas projector of degree k on K_i, $i = 1, 2$. Then,

$$\int_f |\underline{[\![\mathbf{v}]\!]}|^2 \, ds \leq C h_{1,x} \big[\|\partial_x \mathbf{u}\|_{0,K_1}^2 + \|\partial_y \mathbf{u}\|_{0,K_1}^2 \big] + C h_{2,x} \big[\|\partial_x \mathbf{u}\|_{0,K_2}^2 + \|\partial_y \mathbf{u}\|_{0,K_2}^2 \big],$$

with a constant $C > 0$ that is independent of k and the mesh sizes $h_{1,x}$, $h_{2,x}$, $h_{1,y}$, and $h_{2,y}$.

Proof. First, we assume that $\mathbf{u} \in C^\infty(\overline{K}_1 \cup \overline{K}_2)^3$.

For $i = 1, 2$, we denote $\mathbf{u}|_{K_i}$ by $\mathbf{u}^i = (u_x^i, u_y^i, u_z^i)$ and $\mathbf{v}|_{K_i}$ by $\mathbf{v}^i = (v_x^i, v_y^i, v_z^i)$. Since

$$\int_f |\underline{[\![\mathbf{v}]\!]}|^2 \, ds = \int_f (v_x^1 - v_x^2)^2 \, ds + \int_f (v_y^1 - v_y^2)^2 \, ds + \int_f (v_z^1 - v_z^2)^2 \, ds =: T_1 + T_2 + T_3,$$

it is enough to estimate the terms T_1, T_2 and T_3 separately. We observe that $v_x^1 = v_x^2$ (and thus $T_1 = 0$) only if $f = f_1 = f_2$, since the normal component of $\mathbf{v}$ is continuous across f in this case. In the general case, since $u_x^1 = u_x^2$ is continuous across f, we can write

$$\begin{aligned} T_1 &= \int_f (v_x^1 - v_x^2)^2\, ds \le 2\int_{f_1} (u_x^1 - v_x^1)^2\, ds + 2\int_{f_1} (u_x^2 - v_x^2)^2\, ds \\ &\le 2\int_{f_1} (u_x^1 - v_x^1)^2\, ds + 2\int_{f_2} (u_x^2 - v_x^2)^2\, ds := 2T_{1,A} + 2T_{1,B}. \end{aligned}$$

For $T_{1,A}$ we use the representation in Lemma 7.8 of $v_x^1 = \Pi_k^x u_x^1$ on K_1. Lemma 7.1 ensures

$$v_x^1 = (\pi_k^{0,z}\pi_k^{0,y}\pi_{k+1}^{1,x})u_x^1 = (\pi_k^{0,z}\pi_k^{0,y})u_x^1, \quad \text{on } f_1.$$

For the case of $K_1 = \widehat{Q}$, we have

$$\begin{aligned} T_{1,A} &= \int_{f_1} (u_x^1 - \pi_k^{0,z}\pi_k^{0,y}u_x^1)^2\, ds \le \int_{f_1} |u_x^1|^2 ds \\ &= \int_{\hat{I}} dy \int_{\hat{I}} dz\, |u_x^1(x_2, y, z)|^2 \le C\int_{\hat{I}} dx \int_{\hat{I}} dy \int_{\hat{I}} dz\, |\partial_x u_x^1(x, y, z)|^2, \end{aligned}$$

where we have used the stability of the L^2-projection $\pi_k^{0,z}\pi_k^{0,y}$ in Lemma 7.2, and the fact that functions in $H^1(\hat{I})$ are continuous. For a generic K_1 of the form in (42), we employ a scaling argument and obtain

$$\int_{f_1} (u_x^1 - v_x^1)^2\, ds \le Ch_{1,x}\|\partial_x u_x^1\|_{0,K_1}^2.$$

A bound for $T_{1,B}$ can be found in the same way. We obtain

$$T_1 \le C(h_{1,x}\|\partial_x u_x^1\|_{0,K_1}^2 + h_{2,x}\|\partial_x u_x^2\|_{0,K_2}^2). \tag{43}$$

Let us now consider the term T_2. Since $u_y^1 = u_y^2$ on f_1, we have $\pi_k^{0,z}u_y^1 = \pi_k^{0,z}u_y^2$ and can then bound T_2 by

$$\begin{aligned} T_2 &= \int_f (v_y^1 - v_y^2)^2\, ds \le 2\int_{f_1} \left(v_y^1 - \pi_k^{0,z}u_y^1\right)^2 ds + 2\int_{f_1} \left(v_y^2 - \pi_k^{0,z}u_y^2\right)^2 ds \\ &\le 2\int_{f_1} \left(v_y^1 - \pi_k^{0,z}u_y^1\right)^2 ds + 2\int_{f_2} \left(v_y^2 - \pi_k^{0,z}u_y^2\right)^2 ds =: 2T_{2,A} + 2T_{2,B}. \end{aligned}$$

Let us further estimate the term $T_{2,A}$. From the representation in Lemma 7.8 and the stability of $\pi_k^{0,z}$ in Lemma 7.2, we find

$$T_{2,A} = \int_{f_1} \left(\pi_k^{0,z}u_y^1 - (\pi_k^{0,z}\pi_{k+1}^{1,y}\pi_k^{0,x})u_y^1\right)^2 ds \le \int_{f_1} \left(u_y^1 - (\pi_{k+1}^{1,y}\pi_k^{0,x})u_y^1\right)^2 dydz.$$

We now note that $(\pi_{k+1}^{1,y}\pi_k^{0,x})$ is the second component of the two-dimensional Raviart-Thomas interpolant on the shape-regular rectangle $(x_1, x_2) \times (y_1, y_2)$.

We can then use the two-dimensional result in Lemma 7.4 and obtain

$$\begin{aligned} T_{2,A} &\leq \int_{-1}^{1} dz \int_{y_1}^{y_2} dy \left(u_y^1(x_2,y,z) - (\pi_{k+1}^{1,y}\pi_k^{0,x}u_y^1)(x_2,y,z)\right)^2 \\ &\leq Ch_{1,x} \int_{-1}^{1} dz \int_{y_1}^{y_2} dy \int_{x_1}^{x_2} dx \big(|\partial_x \mathbf{u}^1(x,y,z)|^2 + |\partial_y \mathbf{u}^1(x,y,z)|^2\big) \\ &\leq Ch_{1,x} \left[\|\partial_x \mathbf{u}^1\|_{0,K_1}^2 + \|\partial_y \mathbf{u}^1\|_{0,K_1}^2\right]. \end{aligned}$$

A bound for $T_{2,B}$ can be found in the same way. This yields

$$T_2 \leq Ch_{1,x}\left(\|\partial_x \mathbf{u}^1\|_{0,K_1}^2 + \|\partial_y \mathbf{u}^1\|_{0,K_1}^2\right) + Ch_{2,x}\left(\|\partial_x \mathbf{u}^2\|_{0,K_2}^2 + \|\partial_y \mathbf{u}^2\|_{0,K_2}^2\right). \tag{44}$$

For the term T_3, we proceed as for T_1 and write

$$\begin{aligned} T_3 &= \int_f (v_z^1 - v_z^2)^2\,ds \leq 2\int_{f_1}(u_z^1 - v_z^1)^2\,ds + 2\int_{f_1}(u_z^2 - v_z^2)^2\,ds \\ &\leq 2\int_{f_1}(u_z^1 - v_z^1)^2\,ds + 2\int_{f_2}(u_z^2 - v_z^2)^2\,ds := 2T_{3,A} + 2T_{3,B}, \end{aligned}$$

and bound the two last terms separately using the representation of Lemma 7.8. We first note that $u_z^1 = u_z^2 = 0$ at $z = \pm 1$, so that we can use (38) in Lemma 7.2:

$$T_{3,A} = \int_{f_1}\left(u_z^1 - (\pi_{k+1}^{1,z}\pi_k^{0,y}\pi_k^{0,x})u_z^1\right)^2 dydz \leq Ck\int_{f_1}\left(u_z^1 - (\pi_k^{0,y}\pi_k^{0,x})u_z^1\right)^2 dydz.$$

Using the error estimate for the L^2–projection $(\pi_k^{0,y}\pi_k^{0,x})$ on the shape-regular element $(x_1,x_2)\times(y_1,y_2)$ in Lemma 7.7, we find

$$\begin{aligned} T_{3,A} &\leq Ck\int_{-1}^{1} dz \int_{y_1}^{y_2} dy \left(u_z^1(x_2,y,z) - (\pi_k^{0,y}\pi_k^{0,x}u_z^1)(x_2,y,z)\right)^2 \\ &\leq Ch_{1,x}\int_{-1}^{1} dz \int_{y_1}^{y_2} dy \int_{x_1}^{x_2} dx \big(|\partial_x u_z^1(x,y,z)|^2 + |\partial_y u_z^1(x,y,z)|^2\big). \end{aligned}$$

Since a bound for $T_{3,B}$ can be found in the same way, we find

$$T_3 \leq Ch_{1,x}\left(\|\partial_x u_z^1\|_{0,K_1}^2 + \|\partial_y u_z^1\|_{0,K_1}^2\right) + Ch_{2,x}\left(\|\partial_x u_z^2\|_{0,K_2}^2 + \|\partial_y u_z^2\|_{0,K_2}^2\right). \tag{45}$$

For $\mathbf{u} \in C^\infty(\overline{K}_1 \cup \overline{K}_2)^3$ the assertion follows by combining (43), (44), and (45).

The proof is extended to functions $\mathbf{u} \in H^1(\overline{K}_1 \cup \overline{K}_2)^3$ by a density argument. $\square$

In exactly the same manner, using the representation result of Lemma 7.8, we obtain the following bound for the other faces.

Lemma 7.12. *Let K be an element of the form (41) and f an entire face of K. Assume that $ch_x \leq h_y \leq Ch_x$. Let $\mathbf{u} \in H^1(K)^3$ with $\mathbf{u}|_f = \mathbf{0}$, and let $\mathbf{v}$ be the Raviart-Thomas projector of degree k on K. Then we have that*

$$\int_f |\mathbf{v} \otimes \mathbf{n}_K|^2 ds \leq Ch|\mathbf{u}|_{1,K}^2,$$

with $h = h_x \sim h_y$. The constant C is independent of k, and the mesh sizes h_x, and h_y.

Proof. The proof for the lateral faces parallel to the z-axis can be carried out as in the proof of Lemma 7.11. When f is given by $z = \pm 1$, we can use the results in [26, Lemma 6.10] for three-dimensional shape-regular elements and a scaling argument. □

8 Divergence stability on edge patches

Let $\mathcal{T}_e^{n,\sigma}$ be an edge patch on $\widehat{Q}$. We show that $\mathbb{Q}_k - \mathbb{Q}_{k-1}$ elements are stable on such patches with an inf-sup constant of the order $\mathcal{O}(k^{-3/2})$. The main result of this section is the following theorem.

Theorem 8.1. *Let $\mathcal{T}_e^{n,\sigma}$ be an edge patch on $\widehat{Q}$ with a grading factor $\sigma \in (0, 1)$ and n layers of refinement. Let $k \geq 1$. Then*

$$\sup_{0 \neq \mathbf{v} \in \widetilde{\mathbf{V}}_h^k(\mathcal{T}_e^{n,\sigma};\widehat{Q})} \frac{B_{h,\widehat{Q}}(\mathbf{v}, q)}{\|\mathbf{v}\|_{h,\widehat{Q}}} \geq C k^{-3/2} \|q\|_{0,\widehat{Q}}, \qquad q \in Q_h^{k-1}(\mathcal{T}_e^{n,\sigma}; \widehat{Q}),$$

with a constant $C > 0$ that solely depends on σ, but is independent of k, n, and the aspect ratio of the elements in $\mathcal{T}_e^{n,\sigma}$.

Remark 8.1. *We emphasize that the result in Theorem 8.1 holds for $k = 1$, thus including $\mathbb{Q}_1 - \mathbb{Q}_0$ elements. In particular, the same techniques presented here lead to a stability result of $\mathbb{Q}_1 - \mathbb{Q}_0$ elements on irregular geometric meshes in two space dimensions. This case was not covered in [26].*

The proof of Theorem 8.1 is carried out in the next subsections. We first use the results in section 7.4, in order to prove a stability property for the Raviart-Thomas interpolant on edge patches in Corollary 8.1. The proof then relies on the combination of the two weaker stability results in Lemma 8.2 and Lemma 8.3, respectively.

8.1 Stability of Raviart-Thomas interpolants on edge patches

We define the Raviart-Thomas interpolant $\Pi = \Pi^k : H^1(\widehat{Q})^3 \to \mathbf{V}_h^{k+1}(\mathcal{T}_e^{n,\sigma}; \widehat{Q})$ by

$$\Pi \mathbf{u}|_K = \Pi_K^k(\mathbf{u}|_K), \qquad K \in \mathcal{T}_e^{n,\sigma}. \tag{46}$$

We note that $\Pi\mathbf{u}$ has a continuous normal component across elements that match regularly. If the elements match irregularly, the normal component has jumps; see, e.g., [2, Sect. 3.5]. However, if $\mathbf{u} \in H_0^1(\widehat{Q})^3$ then $\Pi\mathbf{u}$ belongs to $\widetilde{\mathbf{V}}_h^{k+1}(\mathcal{T}_e^{n,\sigma}; \widehat{Q})$.

We first note the following stability result.

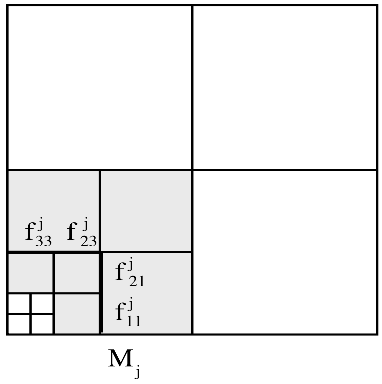

Figure 3: Edge mesh for $\sigma = 0.5$ and $n = 4$. The patch M_j, $j = 3$, is the union of the shaded elements. The four interior faces f^j_{11}, f^j_{21}, f^j_{23} and f^j_{33} in M_j are shown in bold lines.

Theorem 8.1. *Let $\mathcal{T}^{n,\sigma}_e$ be an edge patch on $\widehat{Q}$ with a grading factor $\sigma \in (0,1)$ and n layers of refinement. If $\mathbf{u} \in H^1_0(\widehat{Q})^3$ and $\Pi^k \mathbf{u}$ is the Raviart-Thomas interpolant in (46), then there exists a constant that solely depends on σ, but is independent of k, n, and the aspect ratio of the elements in $\mathcal{T}^{n,\sigma}_e$, such that $\|\mathbf{v}\|^2_{h,\widehat{Q}} \leq Ck^2 |\mathbf{u}|^2_{1,\widehat{Q}}$.*

Proof. This follows by combining Lemma 7.10, Lemma 7.11, Lemma 7.12 and the definition of the penalization function $\delta_{\widehat{Q}}$. □

8.2 Auxiliary stability results

We establish two auxiliary stability results that we need for the proof of our main result in Theorem 8.1.

First we define a seminorm for the space of pressures on edge patches. We consider the interior faces of an edge patch $\mathcal{T}^{n,\sigma}_e$ on $\widehat{Q}$. For $2 \leq j \leq n$, the patch M_j consists of six elements, the cross sections of which are shown in Figure 3. The patch M_1 consists of the four smallest elements of size σ^n. On a patch M_j, $j \geq 2$, the four inner faces will have to be treated separately. We denote them by f^j_{11}, f^j_{21}, f^j_{23} and f^j_{33}, as illustrated in Figure 3.

For $2 \leq j \leq n$, we introduce the seminorm

$$|q|^2_{h,j} = \sum_{i=1,2} h_{f^j_{i1}} \int_{f^j_{i1}} |[\![q]\!]|^2 \, ds + \sum_{i=2,3} h_{f^j_{i3}} \int_{f^j_{i3}} |[\![q]\!]|^2 \, ds.$$

We then set

$$|q|^2_h = \sum_{j=2}^{n} |q|^2_{h,j}. \tag{47}$$

First, we prove the following technical result.

Lemma 8.1. *Let $\mathcal{T}_e^{n,\sigma}$ be an edge patch on $\widehat{Q}$ with a grading factor $\sigma \in (0,1)$ and n layers of refinement. Then there exists a constant that solely depends on σ, but is independent of k, n, and the aspect ratio of the elements in $\mathcal{T}_e^{n,\sigma}$, such that*

$$\left| \int_{\mathcal{E}_\mathcal{I} \cap \widehat{Q}} [\![q]\!] \cdot \{\!\{\mathbf{u} - \Pi^k \mathbf{u}\}\!\}\, ds \right| \le C\, |\mathbf{u}|_{1,\widehat{Q}}\, |q|_h,$$

for $\mathbf{u} \in H^1(\widehat{Q})^3$, $q \in Q_h^k(\mathcal{T}_e^{n,\sigma}; \widehat{Q})$, and $\Pi^k\mathbf{u}$ the interpolant in (46).

Proof. By density, we may assume that $\mathbf{u} \in C^\infty(\overline{\widehat{Q}})^3$. We note that the integral over $\mathcal{E}_\mathcal{I} \cap \widehat{Q}$ can be written as a sum of contributions over faces $f \subset \mathcal{E}_\mathcal{I}$. In addition, if f is a regular face, i.e., it is an entire face of two neighboring elements K and K', then the second orthogonality condition (40) ensures that its contribution vanishes. Indeed, in this case $\mathbf{u}$ and $\Pi^k\mathbf{u}$ have a continuous normal component across f and the normal vector $[\![q]\!]$ belongs to $\mathbb{Q}_{k,k}(f)$. Therefore, we obtain

$$\begin{aligned}\int_{\mathcal{E}_\mathcal{I} \cap \widehat{Q}} [\![q]\!] \cdot \{\!\{\mathbf{u} - \Pi^k \mathbf{u}\}\!\}\, ds &= \sum_{j=2}^{n} \sum_{i=1,2} \int_{f_{i1}^j} [\![q]\!] \cdot \{\!\{\mathbf{u} - \Pi^k \mathbf{u}\}\!\}\, ds \\ &\quad + \sum_{j=2}^{n} \sum_{i=2,3} \int_{f_{i3}^j} [\![q]\!] \cdot \{\!\{\mathbf{u} - \Pi^k \mathbf{u}\}\!\}\, ds.\end{aligned}$$

We first bound the contribution over $f = f_{11}^j$. Denote by K_1 and K_2 the elements that share f, assuming that f is an entire face of K_1. Let q_1 and q_2 be the restrictions of q to K_1 and K_2, respectively. Further, we set $\mathbf{v} = \Pi^k\mathbf{u}$, as well as $\mathbf{u}|_{K_i} = \mathbf{u}^i = (u_x^i, u_y^i, u_z^i)$ and $\mathbf{v}^i = (v_x^i, v_y^i, v_z^i)$ for $i = 1,2$. Therefore,

$$\begin{aligned}\int_f [\![q]\!] \cdot \{\!\{\mathbf{u} - \Pi^k \mathbf{u}\}\!\}\, ds &= \frac{1}{2}\int_f (q_1 - q_2)(u_x^1 - v_x^1)\, ds + \frac{1}{2}\int_f (q_1 - q_2)(u_x^2 - v_x^2)\, ds \\ &= \frac{1}{2}T_1 + \frac{1}{2}T_2.\end{aligned}$$

We start with a bound for T_1 and proceed as in the proof of Lemma 7.11. We use the representation result of Lemma 7.8, the fact that $(q_1 - q_2)$ is a polynomial of degree k in z-direction, the properties of $\pi_k^{0,z}$ and the Cauchy-Schwarz inequality to obtain

$$\begin{aligned}|T_1| &= |\int_f (q_1 - q_2)(u_x^1 - \pi_k^{0,z}\pi_{k+1}^{1,x}\pi_k^{0,y} u_x^1)\, ds| \\ &= |\int_f (q_1 - q_2)(u_x^1 - \pi_{k+1}^{1,x}\pi_k^{0,y} u_x^1)\, ds| \\ &\le \big(h_f \int_f |[\![q]\!]|^2\, ds\big)^{\frac{1}{2}} \big(h_f^{-1} \int_f (u_x^1 - \pi_{k+1}^{1,x}\pi_k^{0,y} u_x^1)^2\, ds\big)^{\frac{1}{2}}.\end{aligned}$$

Since $\pi_{k+1}^{1,x}\pi_k^{0,y}$ is the first component of the two dimensional Raviart-Thomas projector and since the underlying two-dimensional geometric mesh $\mathcal{T}_{xy}^{n,\sigma}$ is shape-regular, we can apply Lemma 7.4 and obtain

$$h_f^{-1} \int_f (u_x^1 - \pi_{k+1}^{1,x} \pi_k^{0,y} u_x^1)^2 \, ds \leq C \|\partial_x \mathbf{u}^1\|_{0,K_1}^2 + C \|\partial_y \mathbf{u}^1\|_{0,K_1}^2.$$

Combining with the analogous argument for T_2 gives

$$\begin{aligned} \left| \int_f [\![q]\!] \cdot \{\!\{\mathbf{u} - \Pi^k \mathbf{u}\}\!\} \, ds \right| &\leq C \big(h_f \int_f |[\![q]\!]|^2 \, ds \big)^{\frac{1}{2}} \\ &\quad \cdot \big(\|\partial_x \mathbf{u}^1\|_{0,K_1}^2 + \|\partial_x \mathbf{u}^1\|_{0,K_1}^2 + \|\partial_x \mathbf{u}^2\|_{0,K_2}^2 + \|\partial_x \mathbf{u}^2\|_{0,K_2}^2 \big)^{\frac{1}{2}}. \end{aligned}$$

The contributions of the other faces f_{ik}^j can be bounded analogously. Summing over all faces and using the Cauchy-Schwarz inequality complete the proof. $\square$

The previous lemma allows us to prove a stability result that is weaker than the inf-sup condition in Theorem 8.1.

Lemma 8.2. *Let $\mathcal{T}_e^{n,\sigma}$ be an edge patch on $\widehat{Q}$ with grading factor $\sigma \in (0,1)$ and n layers of refinement. Then, for $k \geq 1$,*

$$\sup_{0 \neq \mathbf{v} \in \widetilde{\mathbf{V}}_h^k(\mathcal{T}_e^{n,\sigma}; \widehat{Q})} \frac{B_{h,\widehat{Q}}(\mathbf{v}, q)}{\|\mathbf{v}\|_{h,\widehat{Q}}} \geq C k^{-1} \|q\|_{0,\widehat{Q}} \left(1 - \frac{|q|_h}{\|q\|_{0,\widehat{Q}}} \right), \qquad q \in Q_h^{k-1}(\mathcal{T}_e^{n,\sigma}; \widehat{Q}),$$

with a constant $C > 0$ that solely depends on σ, but is independent of k, n, and the aspect ratio of the elements in $\mathcal{T}_e^{n,\sigma}$.

Proof. Let $q \in Q_h^{k-1}(\mathcal{T}_e^{n,\sigma}; \widehat{Q})$. Thanks to the continuous inf-sup condition (3) for $\Omega = \widehat{Q}$, there exists $\mathbf{u} \in H_0^1(\widehat{Q})^3$ such that

$$B(\mathbf{u}, q) = \|q\|_{0,\widehat{Q}}^2, \qquad |\mathbf{u}|_{1,\widehat{Q}} \leq (1/\gamma_\Omega) \, \|q\|_{0,\widehat{Q}}. \tag{48}$$

We choose $\mathbf{v} = \Pi^{k-1} \mathbf{u}$, with Π^{k-1} the interpolant in (46). We then have

$$B_{h,\widehat{Q}}(\mathbf{v}, q) = B(\mathbf{u}, q) - B_{h,\widehat{Q}}(\mathbf{u} - \Pi^{k-1}\mathbf{u}, q) \geq \|q\|_{0,\widehat{Q}}^2 - |B_{h,\widehat{Q}}(\mathbf{u} - \Pi^{k-1}\mathbf{u}, q)|.$$

Using (24) and the first orthogonality property in (40), we can write

$$\begin{aligned} B_{h,\widehat{Q}}(\mathbf{u} - \Pi^{k-1}\mathbf{u}, q) &= \int_{\widehat{Q}} (\mathbf{v} - \Pi^{k-1}\mathbf{u}) \cdot \nabla_h q \, d\mathbf{x} - \int_{\mathcal{E}_\mathcal{I} \cap \widehat{Q}} [\![q]\!] \cdot \{\!\{\mathbf{u} - \Pi^{k-1}\mathbf{u}\}\!\} \, ds \\ &= - \int_{\mathcal{E}_\mathcal{I} \cap \widehat{Q}} [\![q]\!] \cdot \{\!\{\mathbf{u} - \Pi^{k-1}\mathbf{u}\}\!\} \, ds. \end{aligned}$$

Using Lemma 8.1 and the second bound of (48) thus yields

$$B_h(\mathbf{v}, q) = B_h(\mathbf{u}, q) + B_h(\mathbf{v} - \mathbf{u}, q) \geq \|q\|_{0,\widehat{Q}}^2 - C \|q\|_{0,\widehat{Q}} |q|_h. \tag{49}$$

Using Corollary 8.1 and (48) gives

$$\|\mathbf{v}\|_{h,\widehat{Q}} \leq C k |\mathbf{u}|_{1,\widehat{Q}} \leq C k \|q\|_{0,\widehat{Q}},$$

which concludes the proof. $\square$

We end this section by providing a second inf-sup condition in terms of the pressure seminorm $|\cdot|_h$ in (47). Its proof is given in appendix A.

Lemma 8.3. *Let $\mathcal{T}_e^{n,\sigma}$ be an edge patch on $\widehat{Q}$ with a grading factor $\sigma \in (0,1)$ and n layers of refinement. For $k \geq 1$,*

$$\sup_{0\neq \mathbf{v}\in \widetilde{\mathbf{V}}_h^k(\mathcal{T}_e^{n,\sigma};\widehat{Q})} \frac{B_{h,\widehat{Q}}(\mathbf{v},q)}{\|\mathbf{v}\|_{h,\widehat{Q}}} \geq C\,k^{-3/2}|q|_h, \qquad q\in Q_h^{k-1}(\mathcal{T}_e^{n,\sigma};\widehat{Q}),$$

with a constant $C>0$ that solely depends on σ, but is independent of k, n, and the aspect ratio of the elements in $\mathcal{T}_e^{n,\sigma}$.

8.3 Proof of Theorem 8.1

We now combine Lemma 8.2 and Lemma 8.3. If t denotes the ratio $|q|_h/\|q\|_{0,\widehat{Q}}$, we find

$$\sup_{0\neq \mathbf{v}\in \widetilde{\mathbf{V}}_h^k(\mathcal{T}_e^{n,\sigma};\widehat{Q})} \frac{B_{h,\widehat{Q}}(\mathbf{v},q)}{\|\mathbf{v}\|_{h,\widehat{Q}}} \geq Ck^{-3/2}\|q\|_{0,\widehat{Q}}\min_{t\geq 0} f(t), \qquad q\in Q_h^{k-1}(\mathcal{T}_e^{n,\sigma};\widehat{Q}),$$

where $f(t)=\max\{1-t,t\}$. The proof is concluded by noting that the minimum in the inf-sup condition above is equal to $1/2$.

9 Divergence stability on geometric edge meshes

In this section, we consider geometric edge meshes on Ω and prove Theorem 5.1.

9.1 Trivial patch

We have the following result.

Theorem 9.1. *Let $\widehat{\mathcal{T}}$ be the trivial patch given by the mesh $\widehat{\mathcal{T}}=\{\widehat{Q}\}$. For $k\geq 1$,*

$$\sup_{0\neq \mathbf{v}\in \widetilde{\mathbf{V}}_h^k(\widehat{\mathcal{T}};\widehat{Q})} \frac{B_{h,\widehat{Q}}(\mathbf{v},q)}{\|v\|_{h,\widehat{Q}}} \geq C\,k^{-1}\,\|q\|_{0,\widehat{Q}}, \qquad q\in Q_h^{k-1}(\widehat{\mathcal{T}};\widehat{Q}),$$

with a constant $C>0$ independent of k.

Proof. Since $\widehat{\mathcal{T}}$ only consists of one element, given $\mathbf{u}\in H_0^1(\widehat{Q})^3$, we have

$$B_{h,\widehat{Q}}(\Pi_{\widehat{Q}}^{k-1}\mathbf{u},q)=B(\mathbf{u},q), \qquad \|\Pi_{\widehat{Q}}^{k-1}\mathbf{u}\|_{h,\widehat{Q}}\leq Ck|\mathbf{u}|_{1,\widehat{Q}},$$

for all $q\in Q_h^{k-1}(\widehat{\mathcal{T}};\widehat{Q})$, where $\Pi_{\widehat{Q}}^{k-1}$ is the Raviart-Thomas interpolant from section 7.3 on $\widehat{Q}$ and we have used the orthogonality properties in (40) and the results in [26, Lemma 6.9 and Lemma 6.10]. We note that $\Pi_{\widehat{Q}}^{k-1}\mathbf{u}\in\widetilde{\mathbf{V}}_h^k(\widehat{\mathcal{T}};\widehat{Q})$. The divergence stability property is then a consequence of the continuous inf-sup condition (3) for $\Omega=\widehat{Q}$. ☐

9.2 Corner patches

The stability of corner patches is proven by using the macroelement technique.

Theorem 9.2. *Let $\mathcal{T}_c^{n,\sigma}$ be a corner patch on $\widehat{Q}$ with a grading factor $\sigma \in (0,1)$ and n layers of refinement. For $k \geq 2$,*

$$\sup_{0 \neq \mathbf{v} \in \widetilde{\mathbf{V}}_h^k(\mathcal{T}_c^{n,\sigma};\widehat{Q})} \frac{B_{h,\widehat{Q}}(\mathbf{v},q)}{\|\mathbf{v}\|_{h,\widehat{Q}}} \geq C k^{-3/2} \|q\|_{0,\widehat{Q}}, \qquad q \in Q_h^{k-1}(\mathcal{T}_c^{n,\sigma};\widehat{Q}),$$

with a constant $C > 0$ that solely depends on σ, but is independent of k, n, and the aspect ratio of the elements in $\mathcal{T}_c^{n,\sigma}$.

Proof. We use the macroelement technique in Theorem 6.1 and Proposition 6.1 with $\Omega = \widehat{Q}$, the edge mesh $\mathcal{T} = \mathcal{T}_c^{n,\sigma}$ and the macro-element mesh $\mathcal{T}_m = \mathcal{T}_{c,m}^{n,\sigma}$. The stability result (27) for piecewise constant pressures on $\mathcal{T}_m$ then trivially holds by choosing $\mathbf{X}_h$ as the space of continuous, piecewise quadratic velocities; see [31] for regular meshes and [33] for irregular meshes. Condition (35) in Proposition 6.1 is satisfied due to Theorem 9.1 (trivial patch) and by noting that the anisotropically refined elements in $\mathcal{T}_{c,m}^{n,\sigma}$ are particular edge patches that are stable according to Theorem 8.1. $\square$

9.3 Proof of Theorem 5.1

The proof of Theorem 5.1 follows now similarly from the macroelement technique in Theorem 6.1 and Proposition 6.1. Indeed, the low-order stability result (27) on $\mathcal{T}_m$ holds by choosing $\mathbf{X}_h$ again as the space of continuous, piecewise quadratic velocities; see [31]. Condition (35) in Proposition 6.1 is satisfied due to Theorem 9.1 (trivial patch), Theorem 8.1 (edge patch) and Theorem 9.2 (corner patch).

Remark 9.1. *Since we choose the low-order space $\mathbf{X}_h$ in (27) as the space of continuous, piecewise quadratic velocities, Theorem 5.1 and Theorem 9.2 only hold for $k \geq 2$.*

A Proof of Lemma 8.3

We proceed in several steps.

Step 1: A lifting operator. Let $K = K_{xyz} = I_x \times I_y \times I_z$ with $I_x = (x_1, x_2)$ and $h_x = x_2 - x_1$. Consider the face $f_{x_1} = \{x = x_1\}$. We define the operator $\mathcal{E}_{k,K}^{f_{x_1}} : \mathbb{Q}_{k,k}(f_{x_1}) \to \mathbb{Q}_{k+1,k,k}(K)$ by

$$(\mathcal{E}_{k,K}^{f_{x_1}} \varphi)(x,y,z) = M_k^{f_{x_1}}(x)\varphi(y,z), \quad M_k^{f_{x_1}}(x) = \frac{(-1)^{k+1}}{2}(L_{k+1}(x) - L_k(x)),$$

where $\{L_i\}$ here denote the Legendre polynomials on I_x. This lifting operator was originally proposed in [2] and then employed in [26]. Note that

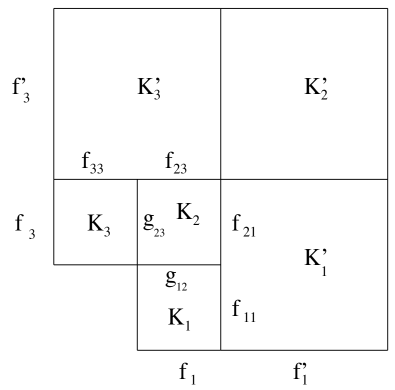

Figure 4: Two-dimensional illustration of the elements and faces in a patch M_j, for $\sigma = 0.5$.

$(\mathcal{E}_{k,K}^{f_{x_1}}\varphi)(x_1, y, z) = \varphi(y, z)$ and $(\mathcal{E}_{k,K}^{f_{x_1}}\varphi)(x_2, y, z) = 0$, thanks to the properties of $\{L_i\}$, cf. [7, Sect. 3]. From the results in [26, Lemma 6.8] and a scaling argument we have

$$\|M_{k,K}^{f_{x_1}}\|_{0,I_x}^2 \leq Ch_x k^{-1}, \qquad |M_{k,K}^{f_{x_1}}|_{1,I_x}^2 \leq Ch_x^{-1}k^3. \tag{50}$$

Analogous definitions and bounds hold for the other faces of K. Furthermore, for $\varphi \in \mathbb{Q}_{k,k}(f_{x_1})$, we have

$$\int_K (\mathcal{E}_{k,K}^{f_{x_1}}\varphi)\, w \, d\mathbf{x} = 0, \qquad \forall w \in \mathbb{Q}^{k-1,k,k}(K). \tag{51}$$

This follows from the definition of the lifting operators and orthogonality properties of the Legendre polynomials. Analogous results are valid for the other faces.

Step 2: Stability on the layer j. Let M_j, $2 \leq j \leq n$, denote the patch of elements illustrated in Figure 3. It consists of 6 elements: we denote the inner elements by K_i, $i = 1, 2, 3$, and the outer ones by K_i', $i = 1, 2, 3$. The four interior faces connecting elements $\{K_i\}$ and $\{K_i'\}$ are denoted by f_{11}, f_{21}, f_{23}, and f_{33}. These faces are entire faces of the inner elements only. The faces connecting the inner elements are g_{12} and g_{23}. The exterior faces are denoted by f_1, f_1' and f_3, f_3', respectively. In Figure 4, we show the configuration of the elements and faces in M_j.

Let $q \in Q_h^{k-1}(\mathcal{T}_e^{n,\sigma}; \widehat{Q})$ for $k \geq 1$. We denote $q|_{K_i}$ by q_i and $q|_{K_i'}$ by q_i', $i = 1, 2, 3$. Using the lifting operators from Step 1, we define the function $\mathbf{v} \in \mathbf{V}_h^k(\mathcal{T}_e^{n,\sigma}; \widehat{Q})$ by

$$\begin{aligned}
\mathbf{v}|_{K_1} = \mathbf{v}^1 &= \big(-h_{f_{11}}\mathcal{E}_{k-1,K_1}^{f_{11}}(q_1 - q_1'), 0, 0\big),\\
\mathbf{v}|_{K_2} = \mathbf{v}^2 &= \big(-h_{f_{21}}\mathcal{E}_{k-1,K_2}^{f_{21}}(q_2 - q_1'), -h_{f_{23}}\mathcal{E}_{k-1,K_2}^{f_{23}}(q_2 - q_3'), 0\big),\\
\mathbf{v}|_{K_3} = \mathbf{v}^3 &= \big(0, -h_{f_{33}}\mathcal{E}_{k-1,K_3}^{f_{33}}(q_3 - q_3'), 0\big),
\end{aligned}$$

and by $\mathbf{v}|_K = \mathbf{0}$ on the remaining elements of $\mathcal{T}_e$. In particular, note that the function $\mathbf{v}$ is equal to zero on the faces adjacent to layer $j+1$ and layer $j-1$ and satisfies $\mathbf{v} \in \widetilde{\mathbf{V}}_h^k(\mathcal{T}_e^{n,\sigma}; \widehat{Q})$.

We first note that $\int_{K_i} \nabla q \cdot \mathbf{v} \, d\mathbf{x} = 0$, $i = 1,2,3$. This follows from the definition of $\mathbf{v}$ and property (51). We define $B_{h,M_j}(\cdot,\cdot)$ and $\|\cdot\|_{0,M_j}$ as in (21) and (22), respectively. Thus,

$$\begin{aligned} B_{h,\widehat{Q}}(\mathbf{v},q) = B_{h,M_j}(\mathbf{v},q) &= -\int_{\mathcal{E}_\mathcal{I} \cap M_j} [\![q]\!] \cdot \{\!\{\mathbf{v}\}\!\} \, ds \\ &= \frac{1}{2} \sum_{i=1,2} \int_{f_{i1}} h_{f_{i1}} |[\![q]\!]|^2 \, ds + \frac{1}{2} \sum_{i=2,3} \int_{f_{i3}} h_{f_{i3}} |[\![q]\!]|^2 \, ds = \frac{1}{2} |q|^2_{h,j}. \end{aligned} \tag{52}$$

Next, we bound the norm $\|\mathbf{v}\|_{h,M_j}$ in terms of $|q|_{h,j}$.

We start by considering the element K_1. Writing $K_1 = I_x \times I_y \times (-1,1)$, we have

$$\|\partial_x \mathbf{v}^1\|^2_{0,K_1} = h^2_{f_{11}} |M^{f_{11}}_{k-1}|^2_{1,I_x} \int_{f_{11}} |[\![q]\!]|^2 \, ds \le C h_{f_{11}} k^3 \int_{f_{11}} |[\![q]\!]|^2 \, ds.$$

Here, we used the second estimate in (50) and the fact that all mesh sizes are comparable in the underlying two-dimensional mesh $\mathcal{T}_{xy}^{n,\sigma}$. Then, from the inverse estimate for polynomials in [27, Theorem 3.91] and the first estimate in (50), we have

$$\begin{aligned} \|\partial_y \mathbf{v}^1\|^2_{0,K_1} &= h^2_{f_{11}} \|M^{f_{11}}_{k-1}\|^2_{0,I_x} \int_{f_{11}} |\partial_y [\![q]\!]|^2 \, ds \\ &\le C h^3_{f_{11}} k^{-1} h^{-2}_{f_{11}} k^4 \int_{f_{11}} |[\![q]\!]|^2 \, ds = C h_{f_{11}} k^3 \int_{f_{11}} |[\![q]\!]|^2 \, ds. \end{aligned}$$

Similarly,

$$\begin{aligned} \|\partial_z \mathbf{v}^1\|^2_{0,K_1} &= h^2_{f_{11}} \|M^{f_{11}}_{k-1}\|^2_{0,I_x} \int_{f_{11}} |\partial_z [\![q]\!]|^2 \, ds \\ &\le C h^3_{f_{11}} k^{-1} k^4 \int_{f_{11}} |[\![q]\!]|^2 \, ds = C h_{f_{11}} k^3 \int_{f_{11}} |[\![q]\!]|^2 \, ds. \end{aligned}$$

Again, we used (50) and the inverse estimate in [27, Theorem 3.91] on the interval $(-1,1)$ in z–direction.

The same techniques yield the analogous estimates for $\mathbf{v}$ on the elements K_2 and K_3. It remains to bound the jumps of $\mathbf{v}$ over the various faces.

We start by considering the jump over f_{11}. Thanks to (16), we have

$$\int_{f_{11}} \delta |\underline{[\![\mathbf{v}]\!]}|^2 \, ds \le C k^2 h^{-1}_{f_{11}} \int_{f_{11}} h^2_{f_{11}} |[\![q]\!]|^2 \, ds = C h^2_{f_{11}} k^2 \int_{f_{11}} |[\![q]\!]|^2 \, ds.$$

The jump over f_{33} can be bounded similarly. Let us now consider the face g_{12}.

Writing $g_{12} = I_x \times \{y_1\} \times (-1,1)$, we have

$$\begin{aligned}
\int_{g_{12}} \delta |\underline{[\![\mathbf{v}]\!]}|^2 \, ds &\leq k^2 h_{g_{12}}^{-1} C \int_{g_{12}} h_{f_{11}}^2 |\mathcal{E}_{k-1,K_1}^{f_{11}}(q_1 - q_1')|^2 \, ds \\
&\quad + k^2 h_{g_{12}}^{-1} C \int_{g_{12}} h_{f_{21}}^2 |\mathcal{E}_{k-1,K_2}^{f_{21}}(q_2 - q_1')|^2 \, ds \\
&\leq Ck^2 h_{f_{11}} \|M_{k-1}^{f_{11}}\|_{0,I_x}^2 \int_{-1}^{1} |[\![q]\!]_{|f_{11}}(y_1,z)|^2 \, dz \\
&\quad + Ck^2 h_{f_{21}} \|M_{k-1}^{f_{21}}\|_{0,I_x} \int_{-1}^{1} |[\![q]\!]_{|f_{21}}(y_1,z)|^2 \, dz \\
&\leq Ckh_{f_{11}}^2 \int_{-1}^{1} |[\![q]\!]_{|f_{11}}(y_1,z)|^2 \, dz + Ckh_{f_{21}}^2 \int_{-1}^{1} |[\![q]\!]_{|f_{21}}(y_1,z)|^2 \, dz \\
&\leq Ck^3 h_{f_{11}} \int_{f_{11}} |[\![q]\!]|^2 \, ds + Ck^3 h_{f_{21}} \int_{f_{21}} |[\![q]\!]|^2 \, ds.
\end{aligned}$$

Here, we used the definition of $\mathbf{v}$, the fact that all mesh sizes are comparable in the underlying two–dimensional mesh $\mathcal{T}_{xy}^{n,\sigma}$, the L^2-bound in (50), and the inverse estimate in [27, Theorem 3.91] for polynomials.

Exactly the same techniques allow us to bound the jumps over g_{23}, f_{23}, f_{21}, f_1 and f_3 in terms of $|q|_{h,j}$. Finally, the same approach gives bounds for the top and bottom faces $z = \pm 1$.

Combining the above estimates yields

$$\|\mathbf{v}\|_{h,\widehat{Q}}^2 = \|\mathbf{v}\|_{h,M_j}^2 \leq Ck^3 |q|_{h,j}^2. \tag{53}$$

Step 3: The assertion. Let $q \in Q_h^{k-1}(\mathcal{T}_e^{n,\sigma}; \widehat{Q})$. On M_j, there is a velocity field $\mathbf{v}_j$ that satisfies (52) and (53). We set $\mathbf{v} = \sum_{j=2}^n \mathbf{v}_j$. By construction, $\mathbf{v} \in \widetilde{\mathbf{V}}_h^k(\mathcal{T}_e^{n,\sigma}; \widehat{Q})$. Using (52), we find

$$B_{h,\widehat{Q}}(\mathbf{v}, q) = \sum_{j=2}^{n} B_{h,\widehat{Q}}(\mathbf{v}_j, q) = \sum_{j=2}^{n} B_{h,M_j}(\mathbf{v}_j, q) \geq C \sum_{j=2}^{m} |q|_{h,j}^2 = C|q|_h^2.$$

Furthermore, from (53) and the fact that the support of the fields $\mathbf{v}_j$ is locally in the patch M_j, we have $\|\mathbf{v}\|_{h,\widehat{Q}}^2 \leq C|q|_h^2$. This concludes the proof.

References

[1] M. Ainsworth and P. Coggins, *The stability of mixed hp–finite element methods for Stokes flow on high aspect ratio elements*, SIAM J. Numer. Anal. **38** (2000), 1721–1761.

[2] M. Ainsworth and K. Pinchedez, *hp-approximation theory for BDFM/RT finite elements and applications*, SIAM J. Numer. Anal., to appear. URL: `http://www.maths.strath.ac.uk/~aas98107/papers/pinch2.ps`.

[3] B. Andersson, U. Falk, I. Babuška, and T. von Petersdorff, *Reliable stress and fracture mechanics analysis of complex aircraft components using a hp–version FEM*, Internat. J. Numer. Methods Engrg. **38** (1995), 2135–2163.

[4] D.N. Arnold, F. Brezzi, B. Cockburn, and L.D. Marini, *Unified analysis of discontinuous Galerkin methods for elliptic problems*, SIAM J. Numer. Anal. **39** (2001), 1749–1779.

[5] I. Babuška and B. Guo, *Approximation properties of the hp–version of the finite element method*, Comput. Methods Appl. Mech. Engrg. **133** (1996), 319–346.

[6] G.A. Baker, W.N. Jureidini, and O.A. Karakashian, *Piecewise solenoidal vector fields and the Stokes problem*, SIAM J. Numer. Anal. **27** (1990), 1466–1485.

[7] C. Bernardi and Y. Maday, *Spectral methods*, Handbook of Numerical Analysis, vol. 5, North-Holland, Amsterdam, 1997, pp. 209–485.

[8] ______, *Uniform inf-sup conditions for the spectral discretization of the Stokes problem*, Math. Models Methods Appl. Sci. **9** (1999), 395–414.

[9] F. Brezzi and M. Fortin, *Mixed and hybrid finite element methods*, Springer Series in Computational Mathematics, vol. 15, Springer–Verlag, New York, 1991.

[10] C. Canuto and A. Quarteroni, *Approximation results for orthogonal polynomials in Sobolev spaces*, Math. Comp. **38** (1982), 67–86.

[11] B. Cockburn, *Discontinuous Galerkin methods for convection-dominated problems*, High-Order Methods for Computational Physics (T. Barth and H. Deconink, eds.), vol. 9, Springer–Verlag, New York, 1999, pp. 69–224.

[12] B. Cockburn, G. Kanschat, and D. Schötzau, *The local discontinuous Galerkin method for the Oseen equations*, Tech. Report 02-05, Department of Mathematics, University of Basel, 2002.

[13] B. Cockburn, G. Kanschat, D. Schötzau, and C. Schwab, *Local discontinuous Galerkin methods for the Stokes system*, SIAM J. Numer. Anal. **40** (2002), 319–343.

[14] B. Cockburn, G.E. Karniadakis, and C.-W. Shu (eds.), *Discontinuous Galerkin methods. Theory, computation and applications*, Lect. Notes Comput. Sci. Eng., vol. 11, Springer–Verlag, New York, 2000.

[15] B. Cockburn and C.-W. Shu, *Runge–Kutta discontinuous Galerkin methods for convection–dominated problems*, J. Sci. Comput. **16** (2001), 173–261.

[16] L. Franca and R. Stenberg, *Error analysis of some Galerkin-least-squares methods for the elasticity equations*, SIAM J. Numer. Anal. **28** (1991), 1680–1697.

[17] K. Gerdes, J.M. Melenk, C. Schwab, and D. Schötzau, *The hp-version of the streamline diffusion finite element method in two space dimensions*, Math. Models Methods Appl. Sci. **11** (2001), 301–337.

[18] V. Girault and P.A. Raviart, *Finite element methods for Navier–Stokes equations*, Springer–Verlag, New York, 1986.

[19] V. Girault, B. Rivière, and M.F. Wheeler, *A discontinuous Galerkin method with non-overlapping domain decomposition for the Stokes and Navier-Stokes problems*, Tech. Report 02-08, TICAM, UT Austin, 2002.

[20] P. Hansbo and M.G. Larson, *Discontinuous finite element methods for incompressible and nearly incompressible elasticity by use of Nitsche's method*, Comput. Methods Appl. Mech. Engrg. **191** (2002), 1895–1908.

[21] P. Houston, C. Schwab, and E. Süli, *Discontinuous hp-finite element methods for advection–diffusion–reaction problems*, SIAM J. Numer. Anal. **39** (2002), 2133–2163.

[22] O.A. Karakashian and W.N. Jureidini, *A nonconforming finite element method for the stationary Navier-Stokes equations*, SIAM J. Numer. Anal. **35** (1998), 93–120.

[23] J.M. Melenk and C. Schwab, *hp–FEM for reaction–diffusion equations, I. Robust exponential convergence*, SIAM J. Numer. Anal. **35** (1998), 1520–1557.

[24] D. Schötzau and C. Schwab, *Mixed hp-FEM on anisotropic meshes*, Math. Models Methods Appl. Sci. **8** (1998), 787–820.

[25] D. Schötzau, C. Schwab, and R. Stenberg, *Mixed hp-FEM on anisotropic meshes, II. Hanging nodes and tensor products of boundary layer meshes*, Numer. Math. **83** (1999), 667–697.

[26] D. Schötzau, C. Schwab, and A. Toselli, *Mixed hp-DGFEM for incompressible flows*, Tech. Report 02-10, Seminar for Applied Mathematics, ETH Zürich, 2002, in press in SIAM J. on Numer. Anal.

[27] C. Schwab, *p- and hp-FEM – Theory and application to solid and fluid mechanics*, Oxford University Press, Oxford, 1998.

[28] C. Schwab and M. Suri, *The p and hp version of the finite element method for problems with boundary layers*, Math. Comp. **65** (1996), 1403–1429.

[29] C. Schwab, M. Suri, and C.A. Xenophontos, *The hp–FEM for problems in mechanics with boundary layers*, Comput. Methods Appl. Mech. Engrg. **157** (1998), 311–333.

[30] R. Stenberg, *Error analysis of some finite element methods for Stokes problem*, Math. Comp. **54** (1990), 495–508.

[31] R. Stenberg and M. Suri, *Mixed hp-finite element methods for problems in elasticity and Stokes flow*, Numer. Math. **72** (1996), 367–389.

[32] A. Toselli, *hp-discontinuous Galerkin approximations for the Stokes problem*, Tech. Report 02-02, Seminar for Applied Mathematics, ETH Zürich, 2002, in press in Math. Models Method. Appl. Sci.

[33] A. Toselli and C. Schwab, *Mixed hp-finite element approximations on geometric edge and boundary layer meshes in three dimensions*, Tech. Report 01-02, Seminar for Applied Mathematics, ETH Zürich, 2001, in press in Numer. Math.

Research Reports

No.	Authors	Title
02-21	D. Schötzau, C. Schwab, A. Toselli	Mixed *hp*-DGFEM for incompressible flows II: Geometric edge meshes
02-20	A. Toselli, X. Vasseur	A numerical study on Neumann-Neumann and FETI methods for *hp*-approximations on geometrically refined boundary layer meshes in two dimensions
02-19	D. Schötzau, Th.P. Wihler	Exponential convergence of mixed *hp*-DGFEM for Stokes flow in polygons
02-18	P.-A. Nitsche	Sparse approximation of singularity functions
02-17	S.H. Christiansen	Uniformly stable preconditioned mixed boundary element method for low-frequency electromagnetic scattering
02-16	S.H. Christiansen	Mixed boundary element method for eddy current problems
02-15	A. Toselli, X. Vasseur	Neumann-Neumann and FETI preconditioners for *hp*-approximations on geometrically refined boundary layer meshes in two dimensions
02-14	Th.P. Wihler	Locking-Free DGFEM for Elasticity Problems in Polygons
02-13	S. Beuchler, R. Schneider, C. Schwab	Multiresolution weighted norm equivalences and applications
02-12	M. Kruzik, A. Prohl	Macroscopic modeling of magnetic hysteresis
02-11	A.-M. Matache, C. Schwab, T. von Petersdorff	Fast deterministic pricing of options on Lévy driven assets
02-10	D. Schötzau, C. Schwab, A. Toselli	Mixed *hp*-DGFEM for incompressible flows
02-09	Ph. Frauenfelder, Ch. Lage	Concepts - An object-oriented software package for partial differential equations
02-08	A.-M. Matache, J.M. Melenk	Two-Scale Regularity for Homogenization Problems with Non-Smooth Fine Scale Geometry
02-07	G. Schmidlin, C. Lage, C. Schwab	Rapid solution of first kind boundary integral equations in $\mathbb{R}^3$
02-06	M. Torrilhon	Exact Solver and Uniqueness Conditions for Riemann Problems of Ideal Magnetohydrodynamics
02-05	C. Schwab, R.-A. Todor	Sparse Finite Elements for Elliptic Problems with Stochastic Data